




5-2017

End-capping Star-like Polycaprolactone with Different Functional Groups and the Interaction with Smooth Muscle Cells

Qingya Zeng

University of Tennessee, Knoxville, qzeng3@vols.utk.edu

Follow this and additional works at: https://trace.tennessee.edu/utk_gradthes

 Part of the [Biology and Biomimetic Materials Commons](#), and the [Polymer and Organic Materials Commons](#)

Recommended Citation

Zeng, Qingya, "End-capping Star-like Polycaprolactone with Different Functional Groups and the Interaction with Smooth Muscle Cells. " Master's Thesis, University of Tennessee, 2017.
https://trace.tennessee.edu/utk_gradthes/4791

This Thesis is brought to you for free and open access by the Graduate School at TRACE: Tennessee Research and Creative Exchange. It has been accepted for inclusion in Masters Theses by an authorized administrator of TRACE: Tennessee Research and Creative Exchange. For more information, please contact trace@utk.edu.

To the Graduate Council:

I am submitting herewith a thesis written by Qingya Zeng entitled "End-capping Star-like Polycaprolactone with Different Functional Groups and the Interaction with Smooth Muscle Cells." I have examined the final electronic copy of this thesis for form and content and recommend that it be accepted in partial fulfillment of the requirements for the degree of Master of Science, with a major in Materials Science and Engineering.

Roberto S. Benson, Major Professor

We have read this thesis and recommend its acceptance:

Kurt E. Sickafus, David J. Keffer

Accepted for the Council:

Dixie L. Thompson

Vice Provost and Dean of the Graduate School

(Original signatures are on file with official student records.)

**End-capping Star-like Polycaprolactone with Different
Functional Groups and the Interaction with Smooth
Muscle Cells**

A Thesis Presented for the

Master of Science

Degree

The University of Tennessee, Knoxville

Qingya Zeng

May 2017

Acknowledgments

I would like to express my sincere gratitude to my thesis committee: Dr. Roberto S. Benson, Dr. Kurt E. Sickafus and Dr. David J. Keffer, for serving on my committee, reviewing my work, and modifying my thesis.

I would like to thank my colleagues and coworkers for their collaboration, assistance, discussion, and friendship: Dr. Xifeng Liu, Anchao Feng, who helped me a lot on the polymer synthesis; Jinbo Dou, who worked with me on the polymer synthesis; Charles, for the discussion both in class and in the lab; Kevin, who worked with me during the summer.

Last but not the least, I would like thank my family, who supported me a lot during my graduate study.

Abstract

Polycaprolactone (PCL) is a PDA-approved biodegradable polymer with excellent biocompatibility and flexibility. My work has been designed to find out how different functional end groups in star-like PCL samples affect the surface properties (such as hydrophilicity, morphology) and bulk properties (such as thermal, mechanical, rheological properties, and crystallization), and consequently the behavior and functions of primary rat aortic smooth muscle cells (SMCs).

I focused on the synthesis of PCL with different functional groups and their characterizations. In chapter 2, PCL samples with four or six hydroxyl end groups were synthesized with different molecular weights ranging from 8,000 to 30,000 g/mol [gram per mole]. The hydroxyl end groups in PCL were converted into carboxyl, methyl, amino, and acrylate groups, with conversion percentage confirmed by nuclear magnetic resonance (NMR) spectra. Thermal properties of these PCL samples were determined with a Differential Scanning Calorimeter (DSC). In chapter 3, the different spherulitic morphologies formed by 4-arm and 6-arm star-like PCL in isothermal crystallization were explored. In chapter 4, the rheological properties of linear and star-like polymers were determined by using a strain controlled rheometer, which aims to find out the dependence of viscosity on frequency and molecular weight. The rheological properties of star like polymers were compared with the linear ones. In chapter 5, cytotoxicity tests of the star-PCL samples using SMCs were performed, and cell study of SMC attachment, spreading, proliferation on the star-PCL samples with different functional groups were also performed.

Table of Contents

Chapter I Introduction and Literature Review	1
1.1 Chemical and physical properties	2
1.2 Synthesize of PCL	3
1.3 Applications of PCL and development.	4
1.4 The Influence of Surface properties on cell behaviors	5
References	8
Chapter II Synthesis and Characterization of the Star-PCL Samples	16
2.1 Introduction	17
2.2 Synthesis of PCL	17
2.2.1 Synthesis of PCL with hydroxyl groups.	17
2.2.2 The grafting of acrylate groups	18
2.2.3 The grafting of methyl groups	19
2.2.4 The grafting of carboxyl groups	19
2.2.5. The grafting of amino groups	20
2.3 Characterization of PCL samples	21
2.3.1 Molecular weight and PDI determined by GPC	21
2.3.2 Chemical structure determined by ATR	22
2.3.3 Chemical structures and synthesis conversion ratios determined by ¹H NMR.	23
2.4 Results and conclusion	29
References	32
Chapter III Surface Morphologies of the Crystallized Star-PCL Samples	34
3.1 Introduction	35
3.2 Experiment section	36
3.3 Results and discussion	37
References	42
Chapter IV Melt Rheological Properties of Linear and Star-PCL Samples	44
4.1 Introduction	45
4.2 Experiment	46
4.2.1 Material used in the experiment	46
4.2.2 Thermal characterization	46
4.2.3 Rheological properties	47
4.3 Results and discussion	47

4.4 Conclusion	52
References	53
Chapter V Cytotoxicity Test and in Vitro Cell Study of the Star-PCL Samples Using Smooth Muscle Cells	54
5.1 Introduction.....	55
5.2 Experiment	55
5.2.1 PCL sample preparation	55
5.2.2 Smooth Muscle Cells (SMCs).....	55
5.2.3 Cytotoxicity tests	56
5.2.4 In vitro cell attachment and proliferation	56
5.3 Results and discussion	57
5.4 Conclusion	61
References	62
Chapter VI Conclusion and Further Work	63
Vita	65

List of Figures

Figure 2-1 The scheme of 4-arm and 6-arm PCL-OH synthesis procedure	18
Figure 2-2 The scheme of acrylate group end-capping procedure	18
Figure 2-3 The scheme of Methyl group end-capping procedure.....	19
Figure 2-4 The scheme of Carboxyl group end-capping procedure	20
Figure 2-5 The scheme of amino group end-capping procedure	20
Figure 2-6 The scheme of N-Boc protection procedure to get amino group end-capping ...	21
Figure 2-7 FTIR-ATR spectra of (a) 4-arm PCL-OH and (b) 6-arm PCL-OH samples	22
Figure 2-8 Chemical structures of the synthesized polymers	23
Figure 2-9 (a) ¹ H NMR spectra of 4-arm PCL-OH, PCL-CH ₃ and PCL-COOH samples (b) ¹ H NMR spectra of 6-arm PCL-OH, PCL-CH ₃ and PCL-COOH samples (c) ¹ H NMR spectra of 4-arm PCL-acrylate samples (d) ¹ H NMR spectra of 6-arm PCL-acrylate samples (e) ¹ H NMR spectra of 4-arm PCL-NH ₂ samples (f) ¹ H NMR spectra of 6-arm PCL-NH ₂ samples.	25
Figure 2-10 The procedure to get PCL-NH ₂ and the ¹ H NMR peak shifting	26
Figure 2-11 (a) DSC curves of 4-arm PCL-OH samples (b) DSC curves of 6-arm PCL-OH samples (c) DSC curves of 4-arm PCL-COOH samples (d) DSC curves of 6-arm PCL-COOH samples (e) DSC curves of 4-arm PCL-CH ₃ samples (f) DSC curves of 6-arm PCL samples (g) DSC curves of 4-arm PCL-acrylate samples (h) DSC curves of 6-arm PCL-acrylate samples (i) DSC curves of 4-arm PCL-NH ₂ samples (j) DSC curves of 6-arm PCL-NH ₂ samples.....	28
Figure 2-12 (a) water contact angle, (b) diiodomethane contact angle and (c) ethylene glycol contact angles on flat polymer surface.....	29
Figure 3-1 Crystalline morphologies of 4-arm 20K samples crystallized at different temperature.....	37
Figure 3-2 Crystalline morphologies of 6-arm 20K samples crystallized at different temperature	38
Figure 3-3 Crystalline morphology of 6-arm 30K samples crystallized at different temperature	39
Figure 3-4 Crystalline morphology of 55K PCL samples on different substrate.	40
Figure 4-1 DSC curves of linear PCL samples with different molecular weights.....	47
Figure 4-2 Strain rate dependence on the viscosity of (a) linear PCL samples with high molecular weight, (b) linear PCL samples with low molecular weight, (c) 4-arm PCL samples (d) 6-arm PCL samples, measured at 140°C.....	49

Figure 4-3 Temperature dependence on zero-shear viscosity of (a) 4-arm samples, (b) 6-arm samples and (c) linear samples measured at 140°C	50
Figure 4-4 Molecular weight dependence on zero-shear viscosity of (a) 4 arm and (b) 6 arm samples at different temperatures and the compared results with (c) linear samples at 140°C.....	51
Figure 5-1 Normalized cell numbers after 1, 2 and 4 days for (a) 4-arm PCL-OH (b) 6-arm PCL-OH (c) PCL-COOH (d) PCL-NH ₂ (e) PCL-acrylate (f) PCL-CH ₃ samples.	58
Figure 5-2 SMCs cell attachment and proliferation on crystallized 4arm-25K PCL films. .	59
Figure 5-3 SMCs cell attachment and proliferation on crystallized 6arm-30K PCL films. .	60

Chapter I Introduction and Literature Review

1.1 Chemical and physical properties

There are a number of biodegradable polymers having been used in the current times. Poly (ϵ -caprolactone) (PCL) is an aliphatic polyester which has been found to be useful in the prosthetic, suture and also in many of drug deliveries^[1]. The IUPAC name for the compound is (1,7)-polyocean-2-one, and also some other names such as 2-oxepenane homo polymer and 6-Caprolactone polymer^[2]. Its CAS number is 24980-41-4, and common abbreviation for the compound is PCL. Density of the compound is 1.145 g/Cm³, and melting point is 60 °C. They are found to exist at the standard state of 25 °C^[3]. It has recently gained prominence in the current times owing to the biomaterial applications of these compounds^[4]. They are relatively inexpensive products that are found to have degradable kinetics to suit specific anatomical sites^[5]. This makes this compound widely useful. Rheology of the compound is found to have wide variety of uses as biomaterial^[6]. The rheological study is to study the flow of mater in liquids or soft state. The plastic flow is found to be deforming based on the elasticity in response to the applied force^[7]. The rheological behavior of the compounds was found to be pronounced when reacted with the extruded starch. This was the case when observed in the off-line capillary rheometer^[8]. The power line model for the compounds was found to have appropriate correction factors. The consistency coefficient K for the starch was found to be significantly higher^[9]. The Starch-PCL nano composite blends were found to have shear-thinning behavior^[10]. This was found to have higher pseudo plasticity than did 100% PCL. The viscosity of the compounds was higher than that of the PCL composite^[11].

These are some of notable features of the PCL. These components have been used for number of commercial applications. There is a need to synthesize the compounds to convert them into compounds that are viable. These have been explained in the subsequent section.

1.2 Synthesize of PCL

The synthesis of PCL is formed by the ring-opening of polymerization of the cyclic monomer-caprolactone. Catalyst such as stannous octoate is used to catalyze the polymerization and is known to have the low molecular weight alcohol which is used to control the molecular weight of the polymers. There are different mechanisms that are used for the polymerization of the PCL^[12]. These are anionic, co-ordination and radical ions. The methods are known to affect the molecular weight, distribution of the molecules and end group composition^[13]. The PCL is found to be a semi-crystalline polymer. The average molecular weight of the PCL compound varies between 3000 to 80000 g/mol. The PCL is soluble in the carbon tetrachloride, benzene, cyclohexane at room temperature^[14], but has lower solubility in the acetone, ethyl acetate, acetonitrile^[15], and is insoluble in alcohol or petroleum ether^[16]. The PCL is blended with a number of other polymers to crack resistance^[17]. Apart from this, the adhesion is used in the combination with the other polymers such as cellulose propionate, polylactic acid, polylactic acid-co-glycolic acid to increase the rate of absorption of the drug release from microcapsules^[18]. This compatibility of the PCL with other polymers depends on the ratio of permeability of the delivery systems in contention^[19]. Copolymers of the PCL is developed using many of monomers of the PVC, diglycolide, valerlactone to name a few^[20]. The physical and mechanical properties of many of the degradable polymers are used and have been investigated.

1.3 Applications of PCL and development.

PCL is a semicrystalline polyester and has numerous uses^[21]. The *in vivo* degradation rate and the drug permeability are found to be very low. The Capronor® is used as a commercial contraceptive that is used for the delivery of the levonorgestrel^[22]. This has been in use for more than 25 years in market^[23]. There are a number of researches that have been undertaken in the current times to address the micro and nanometer scale drug delivery^[24]. Degradation is an issue for the PCL to be used in a wider scale^[25]. Tissue engineering implication of the PCL is numerous. It has low tensile strength and higher elongation^[26]. It is considered as a good elastic biomaterial. The PCL allows for the scaffolds to be formed and is adhered to the microspheres, electron fibers^[27]. It works through the porous networks that are created by porous leaching^[28]. The PCL composite is widely used in various tissue engineering applications. It is particularly used in the engineering of the scaffold for regenerating ligament, bones or skin or even vascular tissues^[29]. The recent advancement of the PCL hybrid scaffold is based on the interfacial tissue engineering^[30]. There are many scaffold regions that are seeded with the appropriate cells that have been harvested from the ligament or the cartilage sources^[31]. There are many complex tissues like interfaced where the bone-ligament interface is found to be regenerated.

Adhesions are unwanted but unavoidable consequence of the surgery especially after trauma surgery. Many researchers have undertaken to address this issue in the healthcare system^[32]. The PCL films served to reduce the postoperative abdominal adhesions that are found in the abdominal wall model^[33]. The film fabrication method is easy to perform. Currently, in the animal studies, it has been found that the PCL films have fewer adhesions than the seprafilm that is used^[34]. This shows that PCL has immense potential to reduce the formation of abdominal adhesions. This potential has been proven in the rat abdominal model^[35].

The PCL is degraded through hydrolysis reaction^[36]. The ester linkages in the physiological conditions are found to be useful. There is a great deal of attention that has been given to the implantable biomaterials. This has been found to have immense use in the long term implantable devices.

PCL has been approved by the FDA for its uses in the human body. Especially, the use of the PCL in formation of the hydrophobic block of the amphiphilic synthetic block copolymers has immense use in the pharmacological applications. Varieties of drugs are currently encapsulated with the PCL beads. This has been used for controlled release and to targeted drug delivery systems. There are major impurities that are found in the medical grades of PCL such as toluene and tin.

In the areas of dentistry, it is used as a component in root canal fillings, and also used for the retreatment purposes. They are made to reach with the heat and dissolved in the solvents such as chloroform. It is also degradable. Owing to this, it is more conducive for the areas of dentistry. However, this is still in the process of development^[37].

1.4 The Influence of Surface properties on cell behaviors

Cell cultures are treated with the polylysine or basic polymers to cause the cell to adhere tightly membrane. The growth is then improved in this process. Collagen or gelatin is found to improve this behavior slightly. The natural and synthetic polymers are in excess of the basic groups. The pH level is balanced for its use^[38].

Research has indicated that the collagen-r-PCL blend is used for novel functional biomimetic nanofibers that are used for achieving the integration between the cells and scaffolds for unique tissue engineering applications^[39].

For tissue bone regeneration, the PCL was used as an important ingredient^[40]. The developed scaffold has unique and superior physical, mechanical, biological properties to make them useful in the bone tissue regeneration^[41].

The surface of nanoparticles can be chemically modified to improve its compatibilities with the matrix. The N-Octadecyl isocyanate was used as a grafting agent. The PCL was used in the nanocomposite film that was reinforced with the sil whiskers that was produced by the film casting^[42]. There were significant differences that was reporting according to the nature of the nanoparticle. It was also found that the chemical treatment improves properties of the nano composite by altering thermal behavior of the compounds^[43].

There was copolymerization of the lactide with the lactone kind of monomers. The functional group of the compound was found to be malic acid. The copolymerization of the lactide with the macromolecular monomer of dextran was analyzed. The cell culture of the technology proved to be efficient in the bulk and surface modification of the PLA in the tissue engineering^[44]. There is influence of hydrophilicity and roughness of the nanofiber meshes (NFMs) for biological performance of the compound^[45]. Despite the morphological similarity the natural extracellular matrix, they are found to contribute to the cellular performance^[46] and should be optimized^[46].

The cell-biomaterial interaction could be influenced by the surface mechanics, surface morphologies and surface chemistry.

Surface mechanics, surface morphological and chemical features are three major aspects that could influence the cell-biomaterial interaction^[47-49]. Smooth muscles(SMCs) and bone cells prefer to attach on surfaces with higher stiffness. The surface roughness could influence cell attachment, proliferation, migration, and gene expression and cell attachment and proliferation could be enhanced on spherulitic polymer surfaces because of the surface roughness

increasement^[50-54]. The functional groups on the surface could influence cell attachment, proliferation by changing the hydrophilicity and protein adsorption of the surface^[55,56].

In the next chapters, PCL with different functional groups will be synthesized and the functional group influence on SMC behavior will be studied.

References

- [1] Maria Ann Woodruff, and Dietmar Werner Hutmacher. "The return of a forgotten polymer— polycaprolactone in the 21st century." *Progress in Polymer Science* 35, no. 10 (2010): 1217-1256.
- [2] MarianneLabet, and Wim Thielemans. "Synthesis of polycaprolactone: a review." *Chemical Society Reviews* 38, no. 12 (2009): 3484-3504
- [3] AsafSugih, , Jan Drijfhout, Francesco Picchioni, Leon PBM Janssen, and Hero J. Heeres. "Synthesis and properties of reactive interfacial agents for polycaprolactone - starch blends." *Journal of Applied Polymer Science* 114, no. 4 (2009): 2315-2326.
- [4] Seema Agarwal, , Joachim Wendorff, and Andreas Greiner. "Use of electrospinning technique for biomedical applications." *Polymer* 49, no. 26 (2008): 5603-5621.
- [5] Jorge M ás, Estell és, Ana Vidaurre, Jos éM. Meseguer Duenas, and Isabel CastillaCort ázar. "Physical characterization of polycaprolactonescaffolds." *Journal of Materials Science: Materials in Medicine* 19, no. 1 (2008): 189-195.
- [6] DietmarHutmacher, Thorsten Schantz, IwanZein, KeeWoei Ng, SweeHin Teoh, and Kim Cheng Tan. "Mechanical properties and cell cultural response of polycaprolactone scaffolds designed and fabricated via fused deposition modeling." *Journal of Biomedical Materials Research* 55, no. 2 (2001): 203-216.
- [7] Shaun Eshraghi, and Suman Das. "Mechanical and microstructural properties of polycaprolactone scaffolds with one-dimensional, two-dimensional, and three-dimensional orthogonally oriented porous architectures produced by selective laser sintering." *ActaBiomaterialia* 6, no. 7 (2010): 2467-2476.

- [8] Boo - Young, Shin, Sang - Il Lee, Young - Sub Shin, Sunder Balakrishnan, and Ramani Narayan. "Rheological, mechanical and biodegradation studies on blends of thermoplastic starch and polycaprolactone." *Polymer Engineering & Science* 44, no. 8 (2004): 1429-1438.
- [9] Haijun Yu, Wenshou Wang, Xuesi Chen, Chao Deng, and Xiabin Jing. "Synthesis and characterization of the biodegradable polycaprolactone - graft - chitosan amphiphilic copolymers." *Biopolymers* 83, no. 3 (2006): 233-242.
- [10] Bora Mavis, Tolga T. Demirtaş, MenemşeGümüşderelioğlu, GüngörGündüz, and ÜnerÇolak. "Synthesis, characterization and osteoblastic activity of polycaprolactone nanofibers coated with biomimetic calcium phosphate." *Acta Biomaterialia* 5, no. 8 (2009): 3098-3111.
- [11] JinhuiZhang, Jia Xu, Hongyan Wang, Weiqun Jin, and Junfeng Li. "Synthesis of multiblock thermoplastic elastomers based on biodegradable poly (lactic acid) and polycaprolactone." *Materials Science and Engineering: C* 29, no. 3 (2009): 889-893.
- [12] Guo Chao, Tao, Zhi Yong Qian, Mei Juan Huang, Bing Kan, Ying Chun Gu, Chang Yang Gong, Jin Liang Yang et al. "Synthesis, characterization, and hydrolytic degradation behavior of a novel biodegradable pH - sensitive hydrogel based on polycaprolactone, methacrylic acid, and poly (ethylene glycol)." *Journal of Biomedical Materials Research Part A* 85, no. 1 (2008): 36-46.
- [13] Zhaodong Wang, , Liuchun Zheng, Chuncheng Li, Dong Zhang, Yaonan Xiao, Guohu Guan, and Wenxiang Zhu. "A novel and simple procedure to synthesize chitosan-graft-polycaprolactone in an ionic liquid." *Carbohydrate polymers* 94, no. 1 (2013): 505-510.
- [14] Jessica Hoskins, and Scott M. Grayson. "Synthesis and degradation behavior of cyclic poly (ϵ -caprolactone)." *Macromolecules* 42, no. 17 (2009): 6406-6413.

- [15] Keri Boduch-Lee, Toby Chapman, Sarah E. Petricca, Kacey G. Marra, and Prashant Kumta. "Design and synthesis of hydroxyapatite composites containing an mPEG-dendritic poly (L-lysine) star polycaprolactone." *Macromolecules* 37, no. 24 (2004): 8959-8966.
- [16] Andrew Korich, Amanda R. Walker, Christopher Hincke, Caitlin Stevens, and Peter M. Iovine. "Synthesis, characterization, and star polymer assembly of boronic acid end - functionalized polycaprolactone." *Journal of Polymer Science Part A: Polymer Chemistry* 48, no. 24 (2010): 5767-5774.
- [17] Xiaoming Li, Rongrong Cui, Lianwen Sun, Katerina E. Aifantis, Yubo Fan, Qingling Feng, Fuzhai Cui, and Fumio Watari. "3D-printed biopolymers for tissue engineering application." *International Journal of Polymer Science* 2014 (2014).
- [18] Young Dae, Kim, and Jun Ho Kim. "Synthesis of polypyrrole–polycaprolactone composites by emulsion polymerization and the electrorheological behavior of their suspensions." *Colloid and Polymer Science* 286, no. 6-7 (2008): 631-637.
- [19] Olivier Coulembier, Philippe Degée, James L. Hedrick, and Philippe Dubois. "From controlled ring-opening polymerization to biodegradable aliphatic polyester: especially poly (β -malic acid) derivatives." *Progress in Polymer Science* 31, no. 8 (2006): 723-747.
- [20] HaeYongKweon, Mi Kyong Yoo, In Kyu Park, Tae Hee Kim, Hyun Chul Lee, Hyun-Sook Lee, Jong-Suk Oh, Toshihiro Akaike, and Chong-Su Cho. "A novel degradable polycaprolactone networks for tissue engineering." *Biomaterials* 24, no. 5 (2003): 801-808.
- [21] Hong Chen, Dongzhong Chen, Quli Fan, and Xuehai Yu. "Synthesis and properties of polyurethane ionomers based on carboxylated polycaprolactone." *Journal of Applied Polymer Science* 76, no. 14 (2000): 2049-2056.

- [22] Barikani, and Mahmood Mohammadi. "Synthesis and characterization of starch-modified polyurethane." *Carbohydrate Polymers* 68, no. 4 (2007): 773-780.
- [23] Amine Harrane, and Mohammad Belbachir. "Synthesis of Biodegradable Polycaprolactone/Montmorillonite Nanocomposites by Direct In - situ Polymerization Catalysed by Exchanged Clay." In *Macromolecular Symposia* 247, no. 1 (2007): 379-384.
- [24] Yoshito Ikada and Hideto Tsuji. "Biodegradable polyesters for medical and ecological applications." *Macromolecular Rapid Communications* 21, no. 3 (2000): 117-132.
- [25] Sambit Sahoo, James Goh Cho-Hong, and Toh Siew-Lok. "Development of hybrid polymer scaffolds for potential applications in ligament and tendon tissue engineering." *Biomedical Materials* 2, no. 3 (2007): 169.
- [26] Andreas Lendlein and Marc Behl. "Shape-memory polymers for biomedical applications." In *Advances in Science and Technology*, vol. 54, pp. 96-102. Trans Tech Publications, 2008.
- [27] Bret Ulery, Lakshmi Nair, and Cato Laurencin. "Biomedical applications of biodegradable polymers." *Journal of polymer science Part B: polymer physics* 49, no. 12 (2011): 832-864.
- [28] Joerg Tessmar and Achim M. Göpferich. "Customized PEG - derived copolymers for tissue - engineering applications." *Macromolecular Bioscience* 7, no. 1 (2007): 23-39.
- [29] Swathi Ravi and Elliot Chaikof. "Biomaterials for vascular tissue engineering." *Regenerative medicine* 5, no. 1 (2010): 107-120.
- [30] Goh Hutmacher, and Teoh. "An introduction to biodegradable materials for tissue engineering applications." *Annals-Academy Of Medicine Singapore* 30, no. 2 (2001): 183-191

- [31] Jamie Ifkovits and Jason Burdick. "Review: photopolymerizable and degradable biomaterials for tissue engineering applications." *Tissue engineering* 13, no. 10 (2007): 2369-2385.
- [32] LalehGhasemi-Mobarakeh, Molamma P. Prabhakaran, Mohammad Morshed, Mohammad-Hossein Nasr-Esfahani, and Seeram Ramakrishna. "Electrospun poly (ϵ -caprolactone)/gelatin nanofibrous scaffolds for nerve tissue engineering." *Biomaterials* 29, no. 34 (2008): 4532-4539.
- [33] Rajesh Vasita and Dharendra S. Katti. "Nanofibers and their applications in tissue engineering." *International Journal of nanomedicine* 1, no. 1 (2006): 15.
- [34] Ying, Wan, Bo Xiao, Siqin Dalai, Xiaoying Cao, and Quan Wu. "Development of polycaprolactone/chitosan blend porous scaffolds." *Journal of Materials Science: Materials in Medicine* 20, no. 3 (2009): 719-724.
- [35] Hoi-Yan Cheung, Kin-Tak Lau, Tung-Po Lu, and David Hui. "A critical review on polymer-based bio-engineered materials for scaffold development." *Composites Part B: Engineering* 38, no. 3 (2007): 291-300.
- [36] Monique Martina and DietmarHutmacher. "Biodegradable polymers applied in tissue engineering research: a review." *Polymer International* 56, no. 2 (2007): 145-157.
- [37] Dharam Persaud-Sharma and Anthony McGoron. "Biodegradable magnesium alloys: a review of material development and applications." In *Journal of Biomimetics, Biomaterials and Tissue Engineering*, vol. 12, pp. 25-39. Trans Tech Publications, 2011
- [38] Darwin Reyes, , Elizabeth M. Perruccio, S. Patricia Becerra, Laurie E. Locascio, and Michael Gaitan. "Micropatterning neuronal cells on polyelectrolyte multilayers." *Langmuir* 20, no. 20 (2004): 8805-8811.

- [39] Zhang, Venugopal, Z-M.Huang, C. T. Lim, and S. Ramakrishna."Characterization of the surface biocompatibility of the electrospun PCL-collagen nanofibers using fibroblasts." *Biomacromolecules* 6, no. 5 (2005): 2583-2589
- [40] CarsonMeredith, Joe - L. Sormana, Benjamin G. Keselowsky, Andr s J. Garc a, Alessandro Tona, Alamgir Karim, and Eric J. Amis. "Combinatorial characterization of cell interactions with polymer surfaces." *Journal of Biomedical Materials Research Part A* 66, no. 3 (2003): 483-490.
- [41] Seyed-Iman Roohani-Esfahani, Saied Nouri-Khorasani, Zufu Lu, Richard Appleyard, and HalaZreiqat. "The influence hydroxyapatite nanoparticle shape and size on the properties of biphasic calcium phosphate scaffolds coated with hydroxyapatite-PCL composites." *Biomaterials* 31, no. 21 (2010): 5498-5509.
- [42] James Anderson, Analiz Rodriguez, and David T. Chang."Foreign body reaction to biomaterials." In *Seminars in immunology* 20, no. 2 (2008): 86-100.
- [43] Gilberto Siqueira, Julien Bras, and Alain Dufresne. "Cellulose whiskers versus microfibrils: influence of the nature of the nanoparticle and its surface functionalization on the thermal and mechanical properties of nanocomposites." *Biomacromolecules* 10, no. 2 (2008): 425-432.
- [44] Shenguo Wang, Wenjin Cui, and JianzhongBei. "Bulk and surface modifications of polylactide." *Analytical and bioanalytical chemistry* 381, no. 3 (2005): 547-556.
- [45] David Butler, Steven A. Goldstein, and FarshidGuilak. "Functional tissue engineering: the role of biomechanics." *Journal of biomechanical engineering*122, no. 6 (2000): 570-575
- [46] Albino Martins, Elisabete D. Pinho, Susana Faria, Iva Pashkuleva, Alexandra P. Marques, Rui L. Reis, and Nuno M. Neves. "Surface modification of electrospunpolycaprolactone nanofiber meshes by plasma treatment to enhance biological performance." *Small* 5, no. 10 (2009): 1195-1206.

- [47] Harbers, G. M.; Grainger, D. W. Cell-Material Interactions: Fundamental Design Issues for Tissue Engineering and Clinical Considerations. In Introduction to Biomaterials; Guelcher, S. A., Hollinger, J. O., Eds.; CRC Press: Boca Raton, FL, 2005; pp 15–45.
- [48] Wong, J. Y.; Leach, J. B.; Brown, X. Q. Balance of chemistry, topography, and mechanics at the cell-biomaterial interface: Issues and challenges for assessing the role of substrate mechanics on cell response. *Surf. Sci.* 2004, 570, 119.
- [49] Saltzman, W. M.; Kyriakides, T. R. Cell Interactions with Polymers. In Principles of Tissue Engineering, 3rd ed.; Lanza, R., Langer, R., Vacanti, J., Eds.; Elsevier Academic Press: San Diego, CA, 2007; pp 279–96.
- [50] Lim, J. Y.; Donahue, H. J. Cell sensing and response to micro- and nanostructured surfaces produced by chemical and topographic patterning. *Tissue Eng.* 2007, 13, 1879.
- [51] Lim, J. Y.; Donahue, H. J. Cell sensing and response to micro- and nanostructured surfaces produced by chemical and topographic patterning. *Tissue Eng.* 2007, 13, 1879.
- [52] Bettinger, C. J.; Langer, R.; Borenstein, J. T. Engineering substrate topography at the micro- and nanoscale to control cell. *Angew. Chem., Int. Ed. Engl.* 2009, 48, 5406.
- [53] Martinez, E.; Engel, E.; Planell, J. A.; Samitier, J. Effects of artificial micro- and nanostructured surfaces on cell behaviour. *Ann. Anat.* 2009, 191, 126.
- [54] Lord, M. S.; Foss, M.; Besenbacher, F. Influence of nanoscale surface topography on protein adsorption and cellular response. *Nano Today* 2010, 5, 66.
- [55] Bahram, V.; Steven J.J.; Julien P. Hydrophobic surfaces for enhanced differentiation of embryonic stem cell-derived embryoid bodies. *PANS* 2008, 105, 38

[56]Yusuke A; Hiroo I. Effects of surface functional groups on protein adsorption and subsequent cell adhesion using self-assembled monolayers. J. Mater. Chem. 2007, 17, 4079-4087.

Chapter II Synthesis and Characterization of the Star-PCL Samples

2.1 Introduction

Poly(ϵ -caprolactone) (PCL) with four or six hydroxyl end groups were synthesized with different molecular weights ranging from 8,000 to 30,000 g/mol using ring-opening polymerization of ϵ -caprolactone (CL) at the presence of an initiator of pentaerythritol or dipentaerythritol, respectively. The molecular weights were controlled by changing the ratio between the initiator and monomer. Based on the hydroxyl group samples, the hydroxyl end groups in PCL were changed into carboxyl, methyl, amino, and acrylate groups, with conversion rates confirmed by the NMR spectra. Fifty samples were synthesized in total. The molecular weight and PDI were determined by GPC. The thermal properties of these PCL samples were determined on a Differential Scanning Calorimeter (DSC). The surface hydrophilicity of the flat disks of the samples was determined by the contact angle test.

2.2 Synthesis of PCL

Five PCL samples with four hydroxyl groups(4-arm PCL-OH) and five samples with six hydroxyl groups(6-arm PCL-OH) were synthesized, and based on the PCL sample, different functional groups were grafted.

2.2.1 Synthesis of PCL with hydroxyl groups.

The synthesis of PCL triols were reported in our group previously [1,2]. PCL with hydroxyl end groups were synthesized via the ring-polymerization of caprolactone at the presence of initiator and catalyst, $\text{Sn}(\text{Oct})_2$. In order to get PCL with four or six hydroxyl groups, pentaerythritol or dipentaerythritol were used as the initiator. The mixture of caprolactone, $\text{Sn}(\text{Oct})_2$ and pentaerythritol or dipentaerythritol was stirred with a magnetic stir and the reaction temperature was 120°C under nitrogen for 12 h. The molecular weights were controlled by changing the ratio between CL and OH groups. The procedures are shown in Figure 2-1.

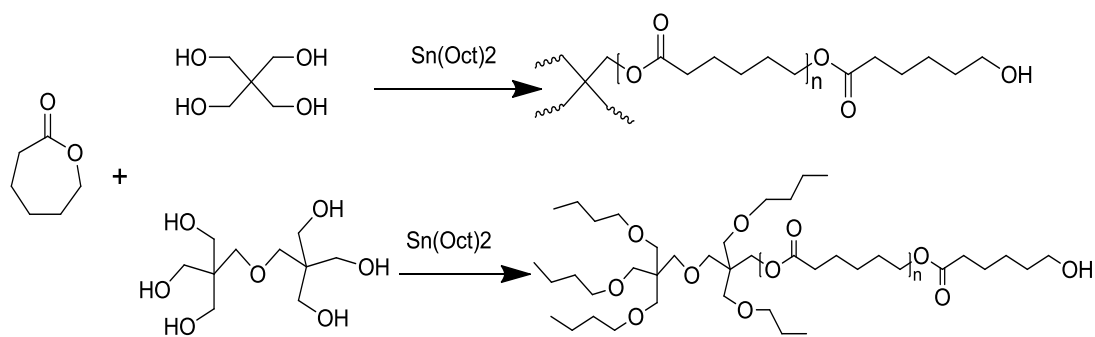


Figure 2-1 The scheme of 4-arm and 6-arm PCL-OH synthesis procedure

2.2.2 The grafting of acrylate groups

The synthesise of PCLTA were also reported in our group previously [1-3]. In order to get acrylate terminated PCL, acryloyl chloride was used for the grafting. Potassium carbonate (K_2CO_3) was used as the proton scavenger. Methylene chloride was used as the solvent. The molar ratio between hydroxyl groups, acryloyl chloride and K_2CO_3 is about 1:1:1. Potassium carbonate was dried in the vacuum drier for 12h and methylene chloride was dried over calcium hydride before using for the reaction. After the reaction under nitrogen at room temperature for 24h, the mixture was precipitated in diethyl ether. The procedures are shown in Figure 2-2.

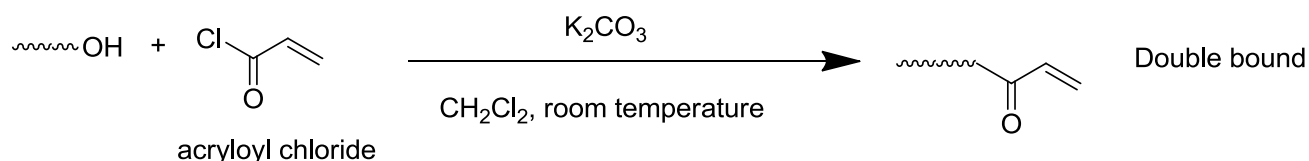


Figure 2-2 The scheme of acrylate group end-capping procedure

2.2.3 The grafting of methyl groups

The procedure to get methyl functional groups grafted based on hydroxyl groups was similar to that to get acrylate end groups, acetyl chloride was used to get the methyl groups end-capping, and K_2CO_3 was used as the proton scavenger. The molar ratio between hydroxyl groups, acetyl chloride and K_2CO_3 is about 1:1:1. Before the reaction happened under nitrogen at room temperature for 24 h, potassium carbonate was dried in the vacuum drier for 12 h and methylene chloride was dried over calcium hydride. After the reaction, the mixture was precipitated in diethyl ether. The procedures are shown in Figure 2-3

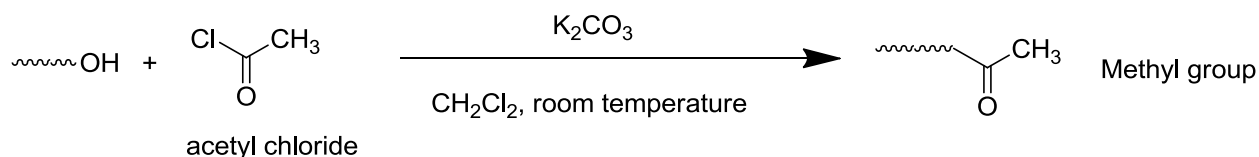


Figure 2-3 The scheme of Methyl group end-capping procedure

2.2.4 The grafting of carboxyl groups

The way to get carboxyl functional groups grafted based on hydroxyl group was reported in Lee's group previously [4]. For the preparation of carboxyl end group samples, methylene chloride solution of PCL-OH and succinic anhydride, 4-Dimethylaminopyridine (DMAP) was added. The molar ratio of hydroxyl groups, DMAP and succinic anhydride is 1:1:1. The reaction happened under nitrogen at room temperature for 24 h. The product, PCL-COOH was isolated by precipitation from the methylene chloride into petroleum ether and then dried in the vacuum dryer at 25°C . The procedures are shown in Figure 2-4.

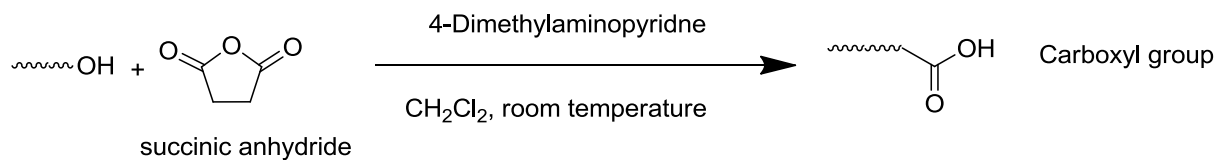


Figure 2-4 The scheme of Carboxyl group end-capping procedure

2.2.5. The grafting of amino groups

It was reported previously on how to convert one hydroxyl into amino end groups [5]. In a two-step procedure, the hydroxyl groups were firstly reacted with 4-nitrophenyl chloroformate to get oxy-nitrophenoxy end groups, and then the oxy-nitrophenoxy end groups further reacted with diamine butane, and thus, the amino group end-capping was achieved. The procedures are shown in Figure 2-5.

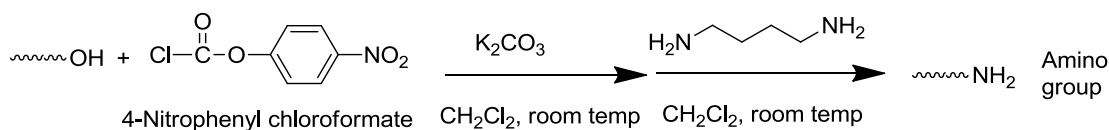


Figure 2-5 The scheme of amino group end-capping procedure

It is an easy way to achieve the amino group convention, however, this method could not be used in my synthesis because there are multiple reactive hydroxyl groups, and as a result, a well crosslinked structure formed in the second step. In order to avoid the crosslinkage, tert-butyloxycarbonyl protecting group (N-BOC group) was introduced, which allows only one amino group converting to the N-Boc group in the second step. In this way, only one amino end group exposed to the environment and could react with the hydroxyl group. After the N-Boc groups were grafted, trifluoroacetic acid (TFA) was used for the deprotection. After the deprotection, the mixture was washed by K_2CO_3 solution to get rid of TFA. A similar synthesise

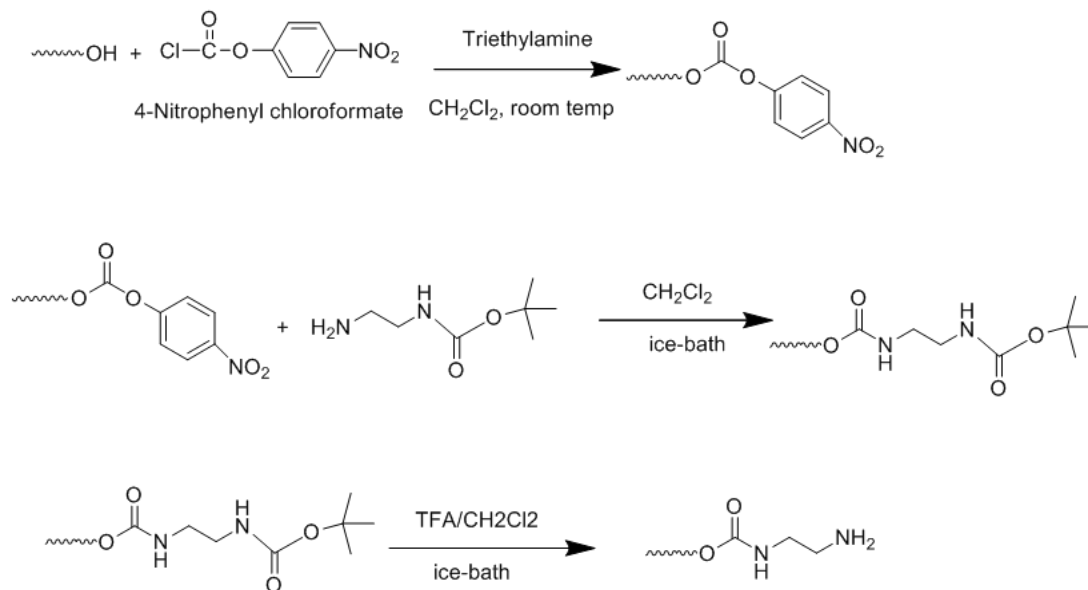


Figure 2-6 The scheme of N-Boc protection procedure to get amino group end-capping

using N-Fmoc group as the protection was talked about in Michele's group [6]. The scheme of the procedure is shown in Figure 2-6.

2.3 Characterization of PCL samples

Molecular weights of the synthesized samples were determined using Gel permeation chromatography (GPC) and structures of the molecules were determined by using ATR and NMR. Based on the NMR spectra, conversion rates were calculated. Thermal properties of these PCL samples were determined on a Differential Scanning Calorimeter (DSC). Surface hydrophilicities of the flat disks prepared by the polymers were determined by contact angle test.

2.3.1 Molecular weight and PDI determined by GPC

Gel permeation chromatography (GPC) was performed at room temperature using a GPC system (HLC-83200GPC, TOSOH Biosciences LLC, Tokyo, Japan) to determine the molecular weight and polydispersity index (PDI) of PCL samples. Tetrahydrofuran (THF) was the used as the

solvent and monodisperse polystyrene samples were used for standard calibration. Cirrus GPC/SEC software (Agilent Technologies, Santa Clara, CA) was used for the data processing.

2.3.2 Chemical structure determined by ATR

Chemical structures were determined by using spectra Attenuated Total Reflectance (ATR) and ^1H Nuclear Magnetic resonance (^1H NMR).

ATR is a infrared spectroscopy like fourier transform infrared spectroscopy (FTIR), but it enabled samples to be tested in a solid state. The ATR spectra were collected with a Perkin Elmer Spectrum Spotlight 300 spectrometer with diamond Attenuated Total Reflectance.

The FTIR-ATR spectra of 4-arm and 6-arm PCL-OH samples are shown in Figure 2-7.

The absorption peaks at 2950 and 2850 cm^{-1} are assigned to asymmetric and symmetric stretching modes of methylene groups ($-\text{CH}_2-$), and the 1740 cm^{-1} is assigned to vibration of $-\text{COOH}$ groups. The FTIR-ATR tests on other samples were also performed; however, compared with the long chain, the peaks that correspond to the functional groups were too weak to observe.

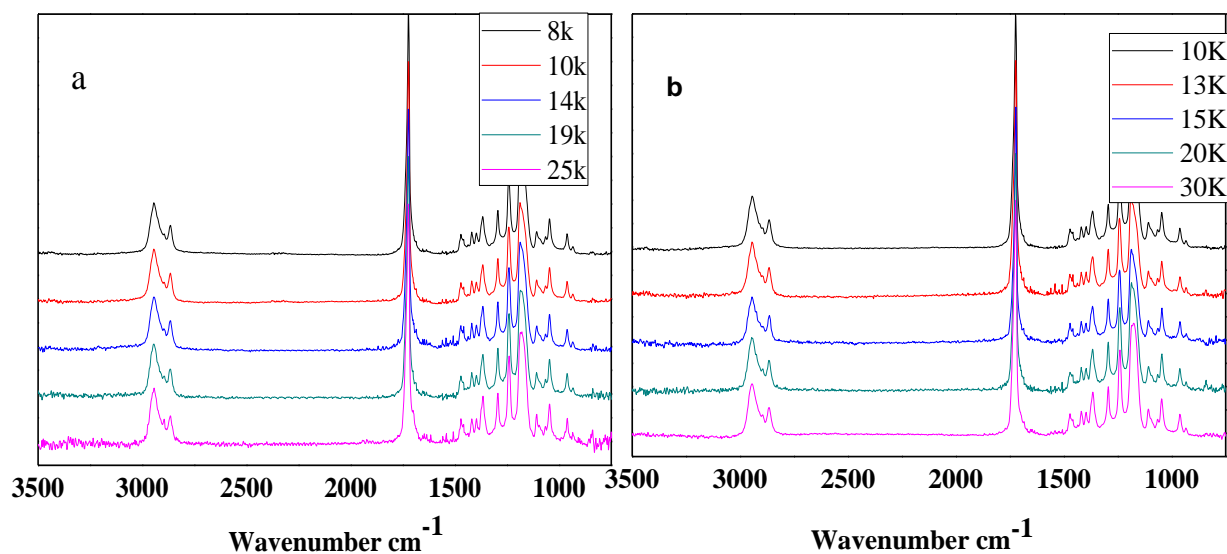


Figure 2-7 FTIR-ATR spectra of (a) 4-arm PCL-OH and (b) 6-arm PCL-OH samples

It was reported in the literature that the $-\text{CH}=\text{CH}_2$ peaks were already very weak when the molecular weight of PCLDA is 2000 [1]. Compared with the weak characteristic peaks on the FTIR-ATR spectra curves, the peaks that correspond to the functional groups could be easily seen on the ^1H NMR spectra curves.

2.3.3 Chemical structures and synthesis conversion ratios determined by ^1H NMR.

Nuclear Magnetic Resonance (^1H NMR) was carried out with a Varian Mercury 300 spectrometer (Agilent Technologies, Santa Clara, CA). CDCl_3 was used as the solvent in the measurement. Software MestReNoVa was used to analyze the ^1H NMR curves and calculate the conversion ratio.

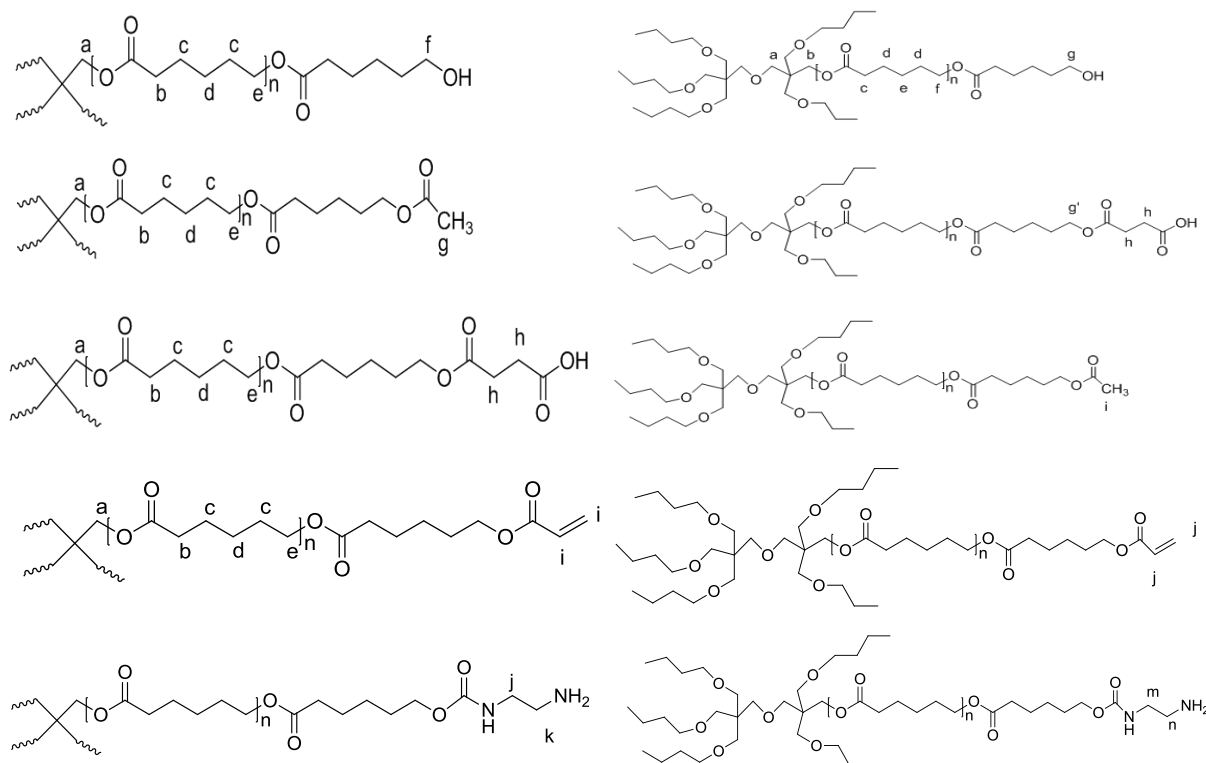


Figure 2-8 Chemical structures of the synthesized polymers

The chemical structures are shown in Figure 2-8 and the ^1H NMR spectra are shown in Figure 2-9, all the corresponding protons are labeled and all the chemical shifts could be observed in the ^1H NMR spectra.

For the PCL-COOH NMR spectra, the resonance at 2.62 ppm in the NMR spectra demonstrates the $-\text{CH}_2\text{CH}_2-$ of terminated carboxyl group, which was reported in Wang's work [7]. For the PCL- CH_3 NMR spectra, the peak at 2.02 ppm indicates the $-\text{CH}_3$ structure. For the PCL-acrylate samples, the peaks ranging from 5.7 to 6.5 ppm demonstrated vinyl groups ($-\text{CH}=\text{CH}-$) in the chemical structure, in agreement with the literature reported [1].

The functional group conversion ratio could be determined by ^1H NMR spectra. When the conversion ratio is 100%, there will be no peak f for functional group terminated PCL. However, there were still weak peaks on the PCL- CH_3 , PCL-COOH and PCL-acrylate ^1H NMR spectra curves. By comparing the peak f and the functional group corresponded peaks, all the conversion ratios of PCL- CH_3 , PCL-COOH and PCL-acrylate samples could be calculated, which are shown in Table 2-1. Most conversion ratios for PCL-COOH samples were above 90%. The conversion ratios for PCL- CH_3 and PCL-acrylate samples were ranging from 80% to 90%.

The synthesis of PCL- NH_2 is a three step procedure. In the first step, the hydroxyl group reacted with 4-Nitrophenyl chloroformate at room temperature. Triethylamine was used as the proton scavenger in this step. In the second step, the PCL-oxy-nitrophenoxy reacted with N-boc and got N-boc group terminated PCL. The N-boc groups were deprotected by using trifluoroacetic acid (TFA) methylene chloride solution in the last step. The mixture was washed with aqueous potassium carbonate then water and dried under vacuum. The scheme of the synthesis procedure, the structures of chemicals and the peak shifting are shown in Figure 2-10.

In the first step, K_2CO_3 was first used as the proton scavenger, but the conversion ratios were very low. Then the triethylamine was used as the proton scavenger and the conversion ratios

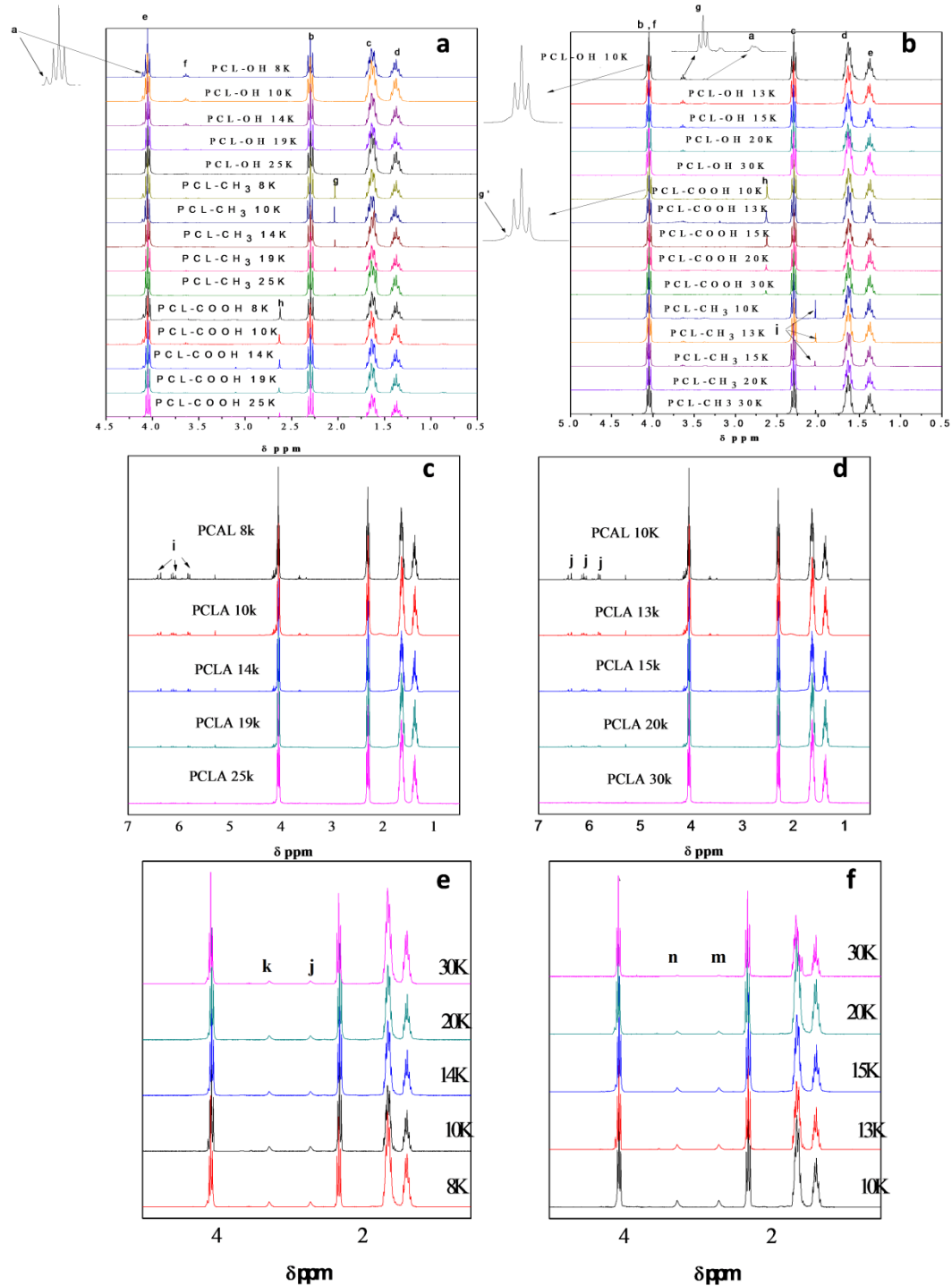


Figure 2-9 (a) ^1H NMR spectra of 4-arm PCL-OH, PCL- CH_3 and PCL-COOH samples (b) ^1H NMR spectra of 6-arm PCL-OH, PCL- CH_3 and PCL-COOH samples (c) ^1H NMR spectra of 4-arm PCL-acrylate samples (d) ^1H NMR spectra of 6-arm PCL-acrylate samples (e) ^1H NMR spectra of 4-arm PCL-NH $_2$ samples (f) ^1H NMR spectra of 6-arm PCL-NH $_2$ samples.

turned out to be almost 100%. In the second step, the conversion ratios were also very high. In the third step, we could see the peak k, which correspond to the N-boc groups, disappeared. However, since the overlapped peaks in the curves, the accurate conversion ratio could not be calculated based on the NMR spectra.

2.3.4 Thermal properties determined by DSC

Thermal properties of 4-arm and 6-arm PCL samples with different functional end groups were determined using a DSC system in a nitrogen atmosphere. All samples were heated from room

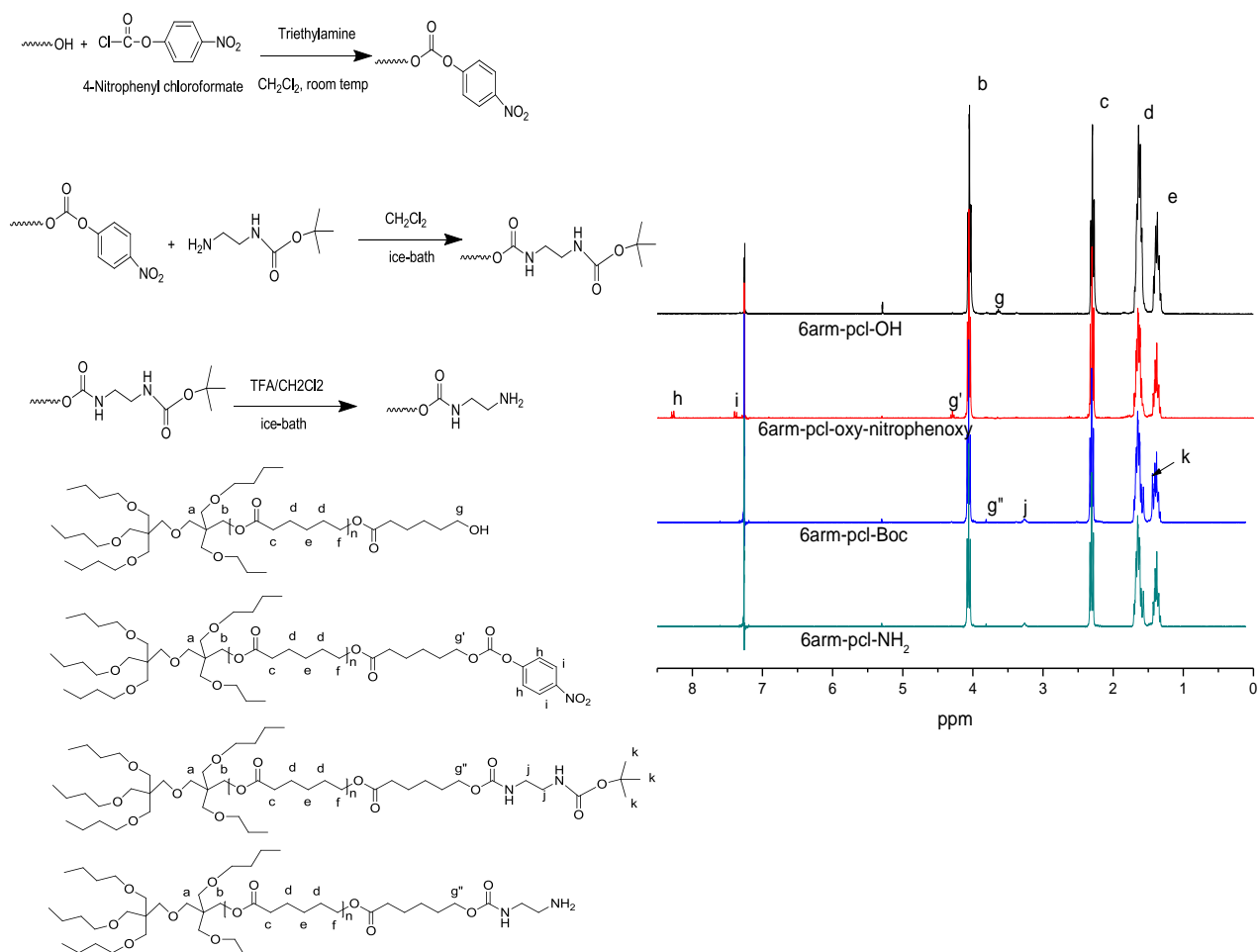


Figure 2-10 The procedure to get PCL-NH₂ and the ¹H NMR peak shifting

temperature to 100°C and then cooled to -60°C at the rate of -10°C/min in order to get same thermal history. After the pretreatment, the samples were heated from 25 °C to 100 °C then cooled to -60 °C at a rate of 10 °C/min. Universal Analysis 2000 software was used to analyze the data. The DSC curves are shown in Figure 2-11. From the heating curves we could get the melting temperature of the samples and from the cooling curve we could get the heat of fusion, which could be used to calculate the crystallinity according to the equation

$$\text{crystallinity}\% = \Delta H_m / (\phi_{PCL} \Delta H_m^c) \quad \text{Where } \Delta H_m^c = 135 \text{ J / g}$$

From the Figure 2-11 we could see that most samples have two melting temperature peaks, which corresponded to the different arm lengths in PCL precursors and PCL samples [1,8]. With the increase of molecular weight (Mn), the crystallization temperature and melting temperature increased a little bit. However, the crystallinity did not change a lot. When different functional groups were compared, the carboxyl group decreased the crystalline temperature significantly; the other end groups did not influence the thermal properties much.

2.3.5 Hydrophilicity

The wettability of the PCL surfaces could be influence by different functional groups on the surface. Hydrophilicity of the samples was determined by contact angle test on flat samples prepared in a hot press. At least three fluids are needed to determine the surface free energy according to the reported method. Pure water, diiodomethane, and ethylene glycol were used in my work. Contact angles were measured with a Ramé-Hart NRC C. A. goniometer (model 100-00-230) at room temperature [9-11]. The contact angles were not recorded until the fluid droplet was stable for more than 30s. The Contact angles of the three fluids on flat surfaces are shown in Figure 2-12.

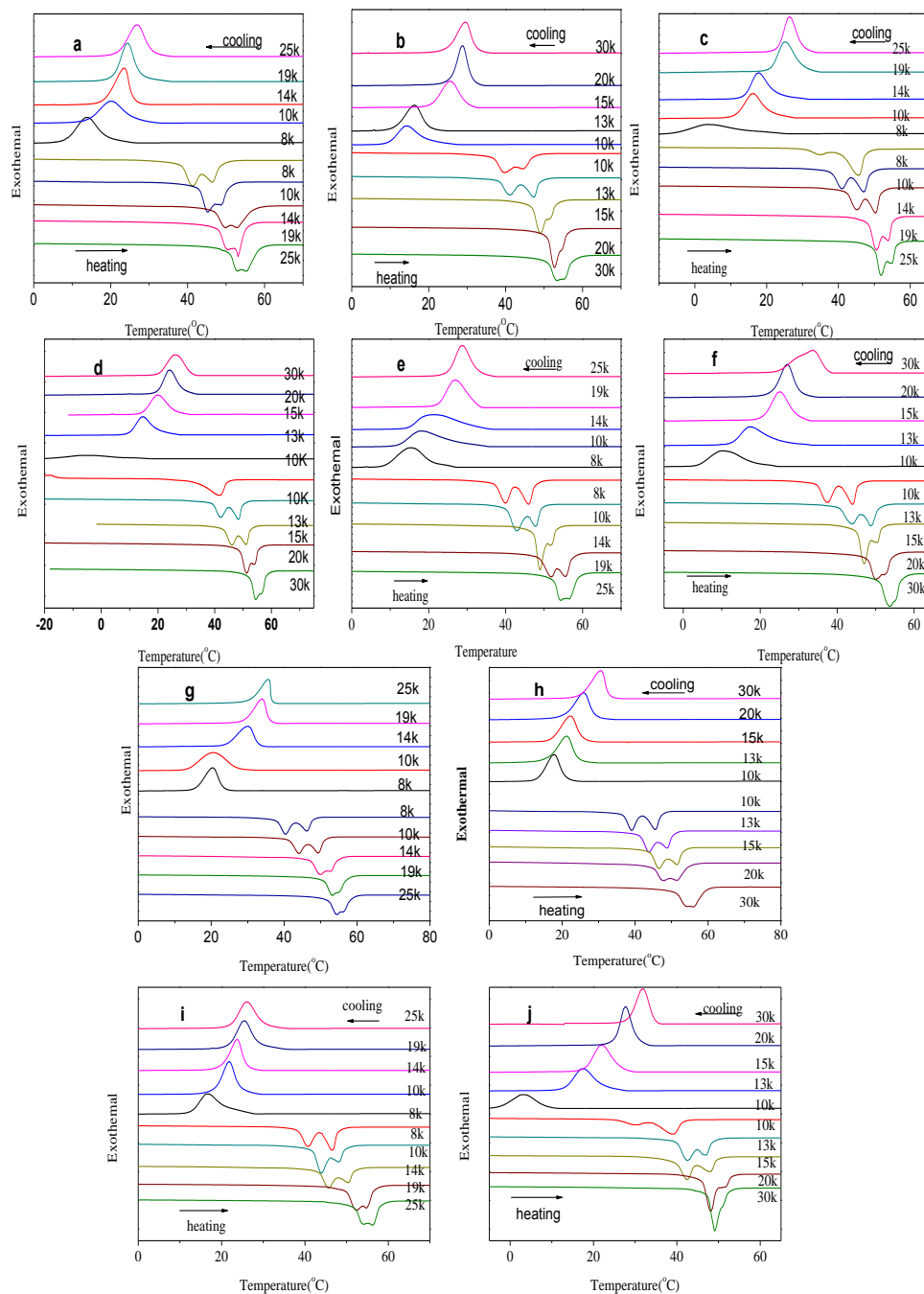


Figure 2-11 (a) DSC curves of 4-arm PCL-OH samples (b) DSC curves of 6-arm PCL-OH samples (c) DSC curves of 4-arm PCL-COOH samples (d) DSC curves of 6-arm PCL-COOH samples (e) DSC curves of 4-arm PCL-CH₃ samples (f) DSC curves of 6-arm PCL samples (g) DSC curves of 4-arm PCL-acrylate samples (h) DSC curves of 6-arm PCL-acrylate samples (i) DSC curves of 4-arm PCL-NH₂ samples (j) DSC curves of 6-arm PCL-NH₂ samples.

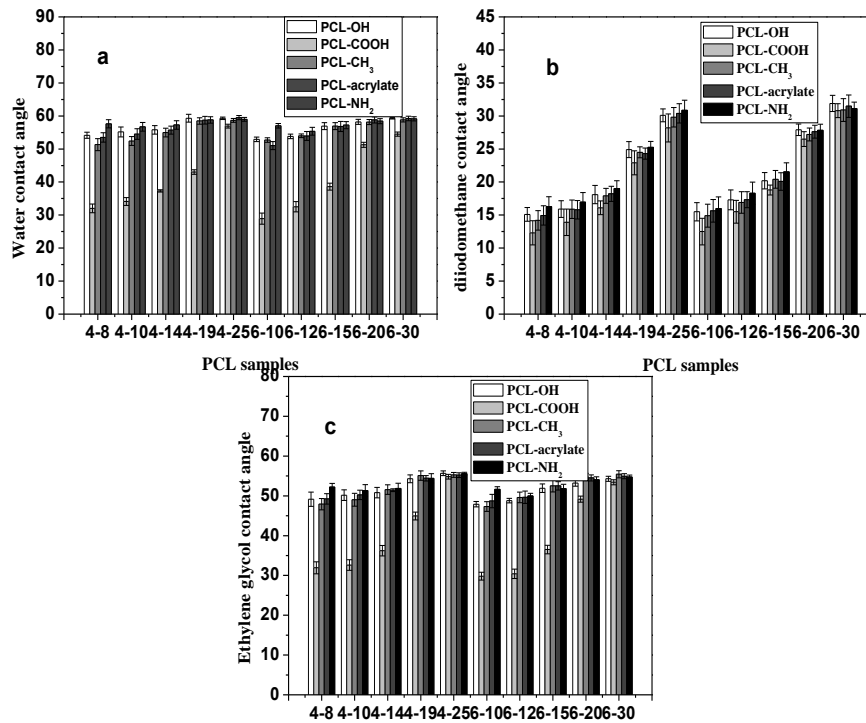


Figure 2-12 (a) water contact angle, (b) diiodomethane contact angle and (c) ethylene glycol contact angles on flat polymer surface.

From the figure we could see that with the increase of molecular weight, water and ethylene glycol contact angles increase a little bit. There is an obvious increase on the diiodomethane contact angles when the molecular weights were increased. The PCL-COOH samples have a much lower contact angle compared with others when all the three fluids were used because the PCL-COOH samples are more hydrophilic. The PCL-NH₂ samples have higher contact angles compared with PCL-OH samples, but not significantly.

2.4 Results and conclusion

Based on the GPC, DSC and NMR, the Molecular weight, PDI, conversion ratio and thermal properties were determined and all the results are shown in the Table 2-1.

From the table we could see the PDI of most samples are about 1.1 except for some high molecular weight samples with the PDI of ~1.3.

The conversion ratios for carboxyl groups were about 90%, which was higher than those of methyl and acrylate groups. The conversion rate could be improved when triethylamine were used as proton scavenger, however, the product turned to be light yellow because of colorization and potential toxicity from the side reaction between TEA and acryloyl chloride, which was reported in our group previously [1].

The crystallization temperature and melting temperature slightly increased when molecular weight increased. The crystallinity did not change much in the molecular weight range. Compared with other samples, the carboxyl end-capping decreased the crystalline temperature significantly; the other end groups have little effects on the thermal properties.

Flat PCL samples with higher molecular weight have higher contact angles when the three fluids were used. Samples with carboxyl groups have lower contact angles compared with the other samples, making the flat surfaces more hydrophilic. X-ray photoelectron spectroscopy (XPS) could be used to further determine the density of functional groups on the flat PCL surfaces.

In the next chapters, these samples will be used for further studies on surface morphologies, rheology properties and cell behaviors.

Table 2-1 Molecular weight characteristics and thermal properties of the functional groups end-capping PCL samples.

Polymer		M _n (g/mol)	M _w (g/mol)	PDI	CR	Thermal properties				
						T _c (°C)	T _{m,1} (°C)	T _{m,2} (°C)	ΔH _m (J/g)	χ _c (%)
PCL-OH	4-8K	8450	9680	1.10		16.60	41.10	46.50	77.80	58.50
	4-10K	9250	10300	1.10		21.00	45.80	49.40	76.60	57.50
	4-14K	14200	15700	1.10		24.20	49.70	52.80	75.30	56.30
	4-19K	19400	22900	1.10		25.00	51.60	54.30	80.50	60.0
	4-25K	28100	36600	1.30		31.40	53.60	55.80	78.50	58.50
	6-10K	9990	10900	1.10		15.10	39.80	44.80	76.20	57.90
	6-13K	12800	14300	1.10		21.80	45.10	48.30	75.30	56.80
	6-15K	15200	16600	1.09		26.71	49.08	51.95	74.53	55.21
	6-20K	17900	20500	1.14		30.78	51.79	54.61	74.99	55.55
	6-30K	29600	37700	1.27		29.93	53.10	55.47	77.85	57.67
PCL-Acrylate	4-8K	7390	8730	1.18	0.82	19.22	40.00	46.30	72.90	55.00
	4-10K	9610	10600	1.10	0.85	20.40	40.40	46.30	73.10	55.00
	4-14K	14700	16700	1.13	0.82	20.40	44.10	49.40	75.50	56.70
	4-19K	19900	23700	1.19	0.91	30.00	50.00	53.00	72.80	54.40
	4-25K	25400	34500	1.36	0.85	35.70	53.20	54.00	72.60	54.10
	6-10K	10200	11200	1.10	0.78	34.00	54.50	56.60	70.50	52.40
	6-13K	13600	14700	1.09	0.79	17.80	39.10	45.60	65.30	49.60
	6-15K	14800	16800	1.14	0.81	20.40	43.90	48.90	70.10	53.00
	6-20K	21000	24800	1.18	0.85	24.30	47.80	51.80	74.10	55.70
PCL-COOH	6-30K	30600	38800	1.27	0.85	30.50	54.00	55.90	67.30	50.30
	4-8K	7880	8730	1.11	0.82	3.320	34.54	45.56	62.31	46.16
	4-10K	9460	10600	1.10	0.81	15.92	40.22	46.45	69.69	51.62
	4-14K	13970	15950	1.14	0.89	17.87	45.45	50.81	72.56	53.75
	4-19K	19800	22900	1.16	0.90	24.82	50.08	53.68	74.52	55.20
	4-25K	27200	35300	1.30	0.90	26.73	51.36	54.64	70.95	52.56
	6-10K	9900	11400	1.15	0.96	-6.28	41.57		31.05	23.00
	6-13K	12800	14300	1.11	0.88	14.33	41.11	47.48	63.92	47.35
	6-15K	15300	16800	1.10	0.90	20.16	45.53	50.7	70.25	52.04
PCL-CH ₃	6-20K	19800	24400	1.24	0.91	24.87	50.44	53.53	67.32	49.87
	6-30K	29900	36600	1.23	0.93	27.89	53.32	55.8	69.78	51.69
	4-8K	8100	8900	1.10	0.87	15.41	39.91	45.98	76.68	56.80
	4-10K	9500	10600	1.10	0.82	18.44	42.87	47.82	75.20	55.70
	4-14K	14800	16500	1.11	0.81	27.86	48.81	52.13	74.38	55.10
	4-19K	19600	23400	1.20	0.85	20.79	50.97	54.94	76.84	56.92
	4-25K	27300	37000	1.36	0.78	28.47	53.80	56.59	73.38	54.36
	6-10K	9800	10800	1.10	0.80	10.31	37.41	44.02	69.12	51.20
	6-13K	12600	14000	1.10	0.85	13.11	43.41	48.49	70.82	52.46
PCL-NH ₂	6-15K	14500	17200	1.14	0.81	24.83	47.50	51.07	73.95	54.78
	6-20K	21600	25200	1.16	0.82	26.95	50.00	53.09	73.28	54.28
	6-30K	31100	36600	1.17	0.86	32.93	53.55	55.16	73.36	54.34
	4-10K	10200	11200	1.10		21.96	43.83	48.30	74.58	55.24
	4-14K	12800	14800	1.13		23.89	45.28	50.18	67.10	49.70
	4-19K	20100	23900	1.19		25.29	51.23	54.03	71.54	52.99
	4-25K	26700	37400	1.40		26.96	53.51	56.36	73.89	54.73
	6-10K	9600	10600	1.10		3.27	29.70	39.07	52.27	38.72
	6-13K	12900	14000	1.10		17.46	42.61	47.38	71.00	52.59
	6-15K	14800	16800	1.13		21.45	42.85	48.77	78.68	58.28
	6-20K	20600	25000	1.18		27.29	47.80	51.44	79.39	58.81
	6-30K	30900	35600	1.15		31.35	49.22		73.70	54.59

References

- [1]. Cai L, Wang S. Poly(ϵ -caprolactone) acrylates synthesized using a facile method for fabricating networks to achieve controllable physicochemical properties and tunable cell responses. *Polymer* 2010;51:164-77.
- [2]. Liu X, Cai L, Hao F, Cui M, Wang S. Biodegradable elastomeric substrates with controllable stiffness for regulating smooth muscle cell behavior. *Polym Mater SciEng* 2011;105:124-6.
- [3]. Cai L, Wang K, Wang S. Poly(ethylene glycol)-grafted poly(propylene fumarate) networks and parabolic dependence of MC3T3 cell behavior on the network composition. *Biomaterials* 2010;31:4457-66.
- [4]. Lee, S. C., et al. "Synthesis and characterization of amphiphilic poly (2-ethyl-2-oxazoline)/poly (ϵ -caprolactone) alternating multiblock copolymers." *Polymer* 41.19 (2000): 7091-7097.
- [5]. Kim, Jae Il, et al. "Examination of phase transition behavior of ion group functionalized MPEG-b-PCL diblock copolymers." *Soft Matter* 7.18 (2011): 8650-8656.
- [6]. Schappacher, Michèle, Alain Soum, and Sophie M. Guillaume. "Synthesis of polyester-polypeptide diblock and triblock copolymers using amino poly (ϵ -caprolactone) macroinitiators." *Biomacromolecules* 7.4 (2006): 1373-1379.
- [7]. Wang, Shanfeng, et al. "Synthesis and characterizations of biodegradable and crosslinkable poly (ϵ -caprolactone fumarate), poly (ethylene glycol fumarate), and their amphiphilic copolymer." *Biomaterials* 27.6 (2006): 832-841.
- [8]. Wang, S.; Lu, L.; Gruetzmacher, J. A.; Currier, B. L.; Yaszemski, M. J. A biodegradable and crosslinkable multiblock copolymer consisting of poly(propylene fumarate) and poly(ϵ -caprolactone): Synthesis, characterization, and physical properties. *Macromolecules* 2005, 38, 7358.
- [9]. O'Connel, C.; Sherlock, R.; Ball, M. D.; Aszalos-Kiss, B.; Prendergast, U.; Glynn, T. J. *Appl. Surf. Sci.* **2009**, 255, 4405.

- [10]. Lampin, M.; Warocquier-Clerout, R.; Legris, C.; Degrange, M.; Sigot-Luizard, M. *F. J Biomed Mater Res.* **1997**, *36*, 99.
- [11]. Harnett, E. M.; Alderman, J.; Wood, T. *Colloids and Surfaces B: Biointerfaces* **2007**, *55*, 90.

Chapter III Surface Morphologies of the Crystallized Star-PCL Samples

3.1 Introduction

Surface mechanics, surface chemistry and morphological features are three major aspects that could influence the cell-biomaterial interaction [1-3]. The surface roughness could influence cell attachment, proliferation, migration, and gene expression and cell attachment and proliferation could be enhanced on spherulitic polymer surfaces because of the surface roughness increasement [4-8]. Most polymers are semi-crystalline, the spherulite contains amorphous part and crystallized polymer lamellar. The polarized optical microscopy (POM) is often used to observe spherulites and the Maltese cross could be observed between the crossed nicols since spherulites are optically anisotropic objects [9]. The impeded polymer crystalline rate and strong surface stress lead to the twisting of the crystallized polymer lamellar and result in the formation of banded structure [10,11].

The following research explores the different spherulitic morphologies formed by 4-arm and 6-arm star-like poly(ϵ -caprolactone) (PCL) in isothermal crystallization. Specifically, we used the samples of PCL with the functional end groups of -OH, -CH₃, -COOH, -CH=CH₂ and -NH₂ to test the effects of molecular weight, crystallization temperature (T_c), different end groups and different substrate.

POM was used to collect images of the spherulites for each sample that were then analyzed using the IC Measure software. Results from each test showed that the increase of T_c increased crystallization time and spherulite area. The samples of PCL with the functional end groups of -COOH and -OH were seen to form a layering morphology over a certain T_c range. Because of this layering, the film was ununiformed, but through an increase in T_m and film thickness, we were able to minimize the layers found in the sample. In addition, -CH₃ and -CH=CH₂ samples were able to form uniform banded spherulites over a T_c range close to the T_m of the polymer. The

PCL was also crystallized on different substrates like glass, Teflon and crosslinked PCLTA, and results showed that the samples formed very good spherulites only on the glass substrate.

3.2 Experiment section

3.2.1 Material used in the experiment

4-arm 25K PCL samples with functional end groups of $-OH$, $-CH_3$, $-COOH$, $-CH=CH_2$, and $-NH_2$ were used to determine how the functional groups and crystalline temperature could affect the crystalline morphology.

6-arm 20K and 6-arm 30K were also used to determine how the molecular weight could influence crystalline morphology.

55K PCL sample (purchased from the Sigma-Aldrich Co.) was used to study how substrate could influence crystalline morphology. The 10K photo-crosslinked poly(ϵ -caprolactone) triacrylate (PCLTA) was synthesized according to a reported procedure [12].

3.2.2 Sample preparation of spin coated thin films.

Solutions of the PCL samples were prepared by dissolving 0.5g of polymer in 5ml of methylene chloride. About 150 microliters of the polymer solution was dropped onto a round glass cover-slip (15mm, diameter) and was spin-coated at a spin rate of 1000 rpm for 20 seconds at room temperature. After the polymer films were fully dried, the polymers were melted on a hot stage at $80^\circ C$ for 10min and quickly transferred to a hot stage with a specific temperature. Room temperature, 37 , 45 and $50^\circ C$ tests were performed to see how the temperature could influence crystalline morphology.

POM pictures were taken when the growing of crystalline structure stops.

3.2.3 Sample preparation of crosslinked PCLTA

Photo-initiator phenyl bis(2,4,6-trimethyl benzoyl) phosphine oxide (BAPO, IRGACURE 819) was supplied by Ciba Specialty Chemicals (Tarrytown, NY). PCLTA and BAPO were dissolved in distilled THF at 50 and 0.5 mg/mL, respectively. The PCLTA/BAPO solution was cast on a clean glass slide and covered with another glass slide for preparing thin PCLTA films (thickness, ~ 1mm) with flat surfaces, followed by gradual drying in air. After the films were dried, they were exposed to UV light ($\lambda= 315\text{-}380\text{ nm}$) for 30 min.

3.3 Results and discussion

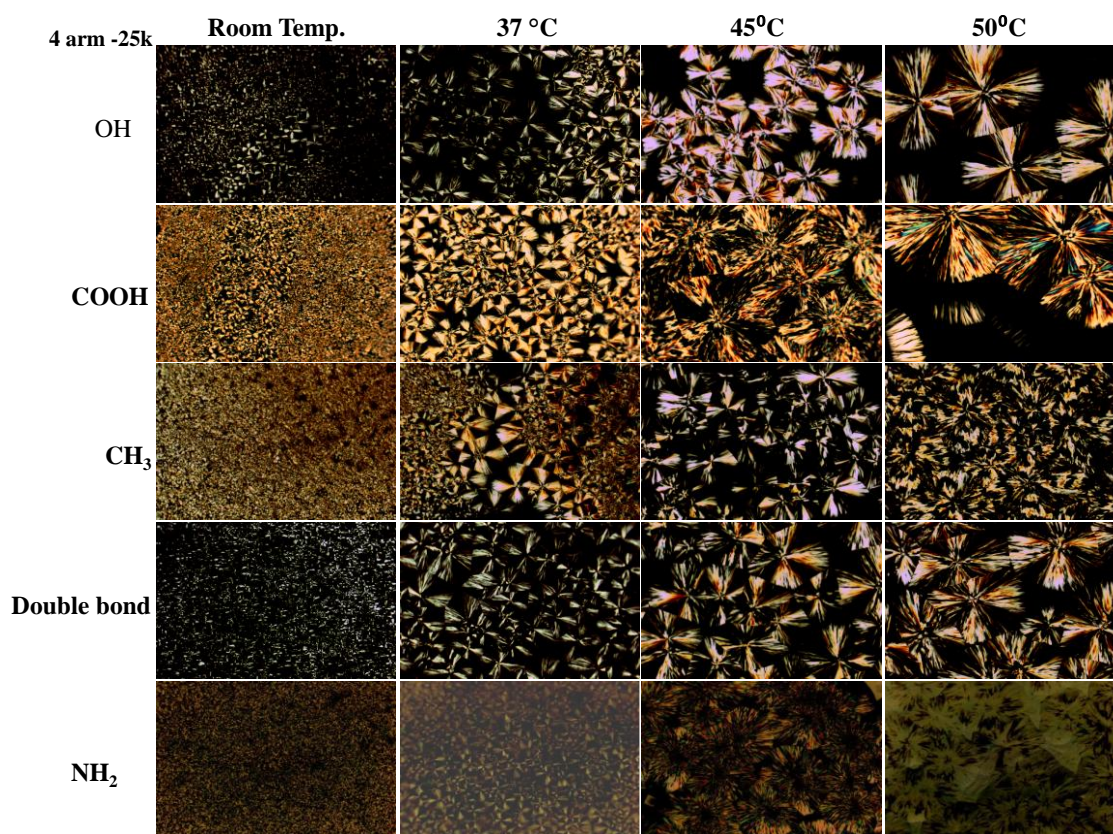


Figure 3-1 Crystalline morphologies of 4-arm 20K samples crystallized at different temperature.

From images in figure 3-1 we can see that at room temperature, only very tiny spherulites formed; with increase of T_c , the speed of crystallization decreased, and larger spherulites formed. A problem for the -OH and -COOH groups was that the spherulites could not fully cover the glass slides and multilayers could also be observed. Because of this layering, the formed film was ununiformed, but through an increase of the heating plate (where the polymer film were heated before transferred to the hot stage) temperature and film thickness, we were able to minimize the layers found in the sample. -CH₃ and -CH=CH₂ samples were able to form uniform banded spherulites when the crystalline temperature was close to melting temperature. Banded structures were not found in the -NH₂ group samples.

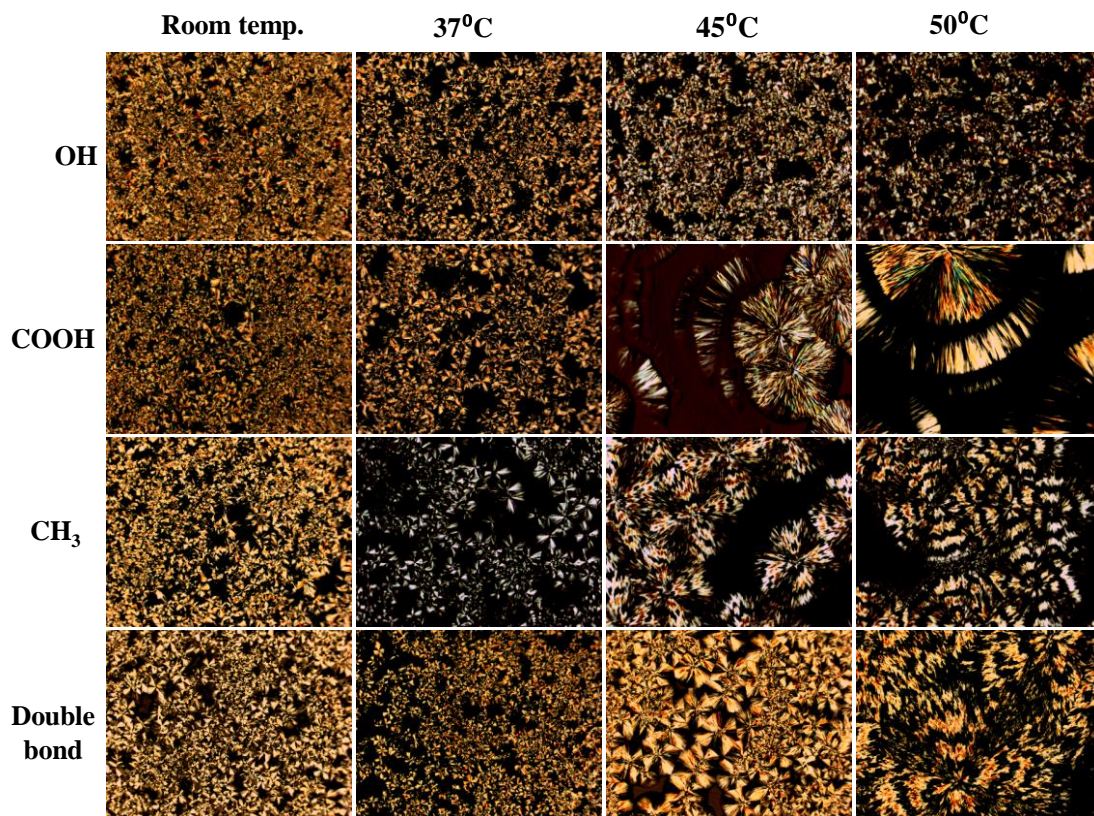


Figure 3-2 Crystalline morphologies of 6-arm 20K samples crystallized at different temperature

Further studies were performed by using 6-arm 20K and 6-arm 30K samples to investigate if the banded structure could form on the same situation. The POM images were shown in Figure 3-2 and Figure 3-3. At the same time, the morphologies difference formed by samples with different molecular weights was compared.

From the images we can see that the when PCL-CH₃ and PCL-acrylate samples were crystallized at 50°C, banded spherulites were observed. PCL-COOH samples formed very good, large spherulites when crystallized at 50°C, but still multi layers were formed.

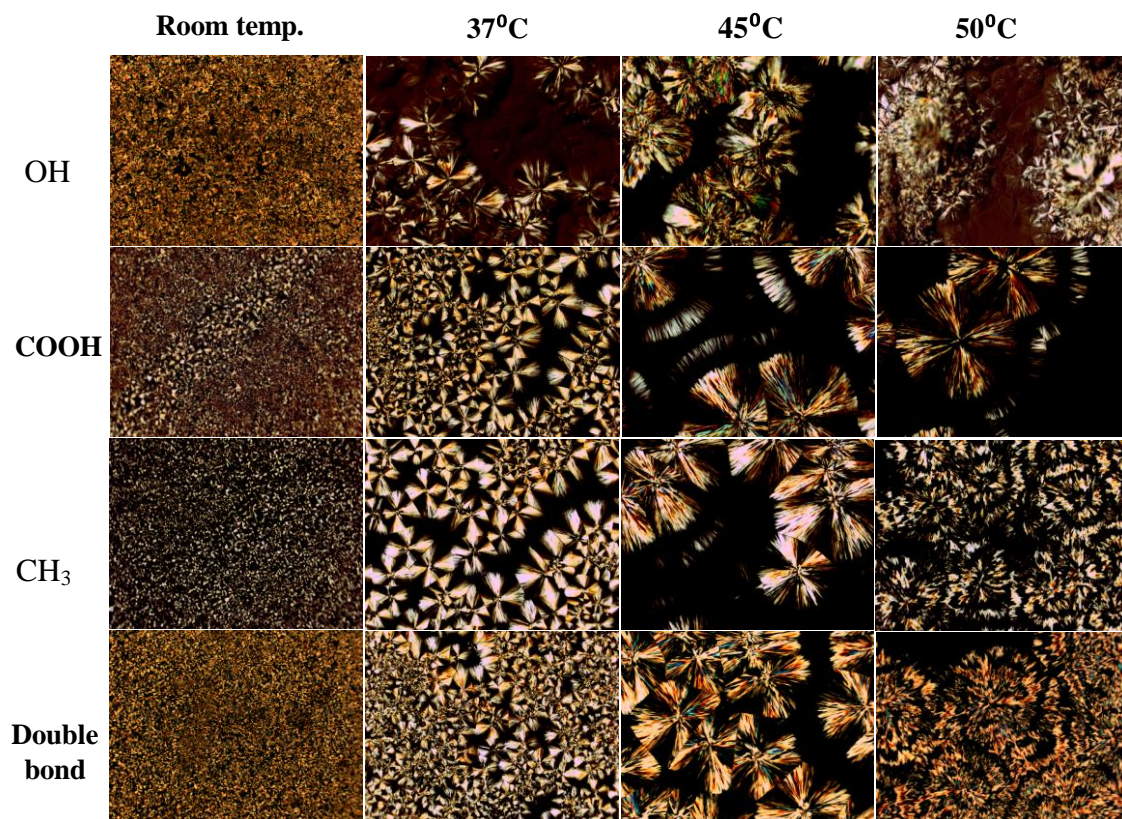


Figure 3-3 Crystalline morphology of 6-arm 30K samples crystallized at different temperature

Comparing with the 6-arm 20K and 6-arm 30K samples, the 6-arm 20K samples formed larger and better spherulites. This could attribute to the melting temperature difference. The melting temperatures of 6-arm 20K samples are lower than those of the 6-arm 30K samples. As a result, when the crystallization happened at a same temperature which is close to the melting temperature, $T_m - T_c$ is smaller for 6-arm 20K samples. The crystalline structure for 6-arm 20K samples were growing slower in comparison with 6-arm 30K samples but larger spherulites were formed at last.

The POM images of crystalline morphologies of 55k PCL samples on glass, Teflon and Crosslinked PCLTA substrates were shown in Figure 3-4.

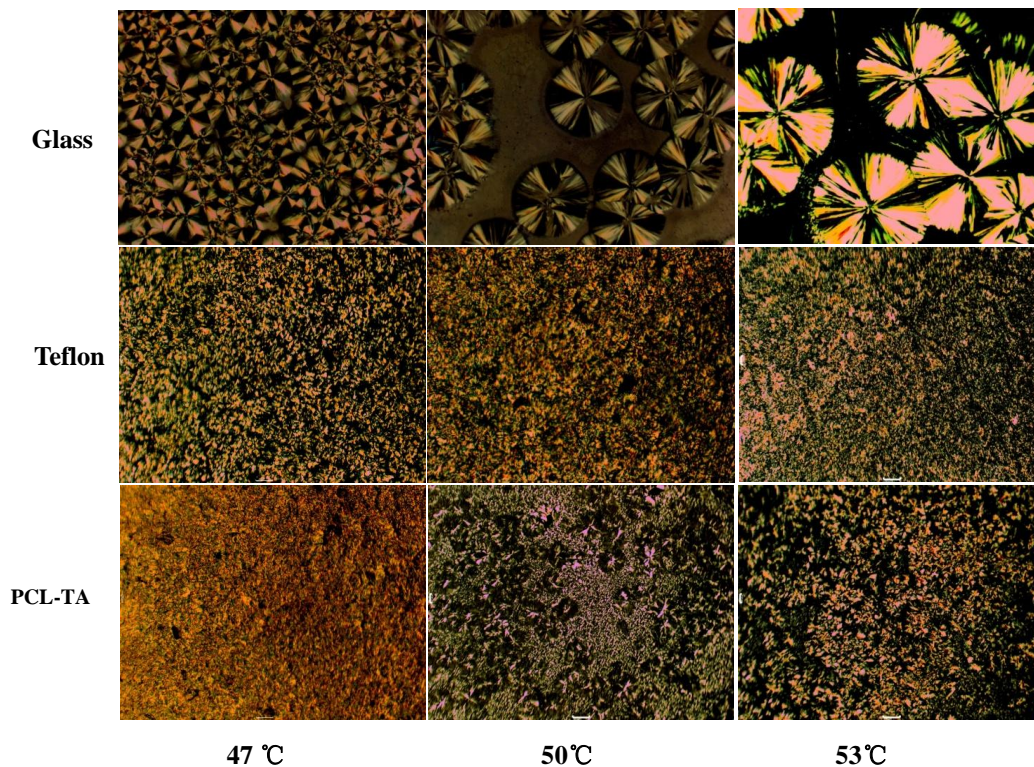


Figure 3-4 Crystalline morphology of 55K PCL samples on different substrate.

From the images we can see large spherulites could only be observed when the samples were crystallized on the glass substrate.

The spherulite were not observed when PCL samples were crystallized on Teflon and PCL-TA substrates, this could either because no spherulites formed or the films were too thick and blocked the light since the samples were prepared by drop coating.

3.4 Conclusion

In this chapter, different functional group end-capping PCL samples were used to study the crystalline morphologies at different temperature and the crystalline morphologies were observed by using POM. Banded structure were observed when the PCL-CH₃ and PCL-acrylate samples were crystallized at 50°C.

When PCL were crystallized on different substrates, no banded structure were observed. Different substrates could influence the crystallization speed of the samples, this part worth further study to find out how could the substrate influence the crystallization.

Crystallization kinetics could be studied by taking the images every specific time for further understanding the crystallinity procedure. Atomic force microscope (AFM) could also be used to further study the roughness of the crystallized surface.

References

- [1]. Harbers, G. M.; Grainger, D. W. Cell-Material Interactions: Fundamental Design Issues for Tissue Engineering and Clinical Considerations. In Introduction to Biomaterials; Guelcher, S. A., Hollinger, J. O., Eds.; CRC Press: Boca Raton, FL, 2005; pp 15–45.
- [2]. Wong, J. Y.; Leach, J. B.; Brown, X. Q. Balance of chemistry, topography, and mechanics at the cell-biomaterial interface: Issues and challenges for assessing the role of substrate mechanics on cell response. *Surf. Sci.* 2004, 570, 119.
- [3]. Saltzman, W. M.; Kyriakides, T. R. Cell Interactions with Polymers. In Principles of Tissue Engineering, 3rd ed.; Lanza, R., Langer, R., Vacanti, J., Eds.; Elsevier Academic Press: San Diego, CA, 2007; pp 279–96.
- [4]. Lim, J. Y.; Donahue, H. J. Cell sensing and response to micro- and nanostructured surfaces produced by chemical and topographic patterning. *Tissue Eng.* 2007, 13, 1879.
- [5]. Lim, J. Y.; Donahue, H. J. Cell sensing and response to micro- and nanostructured surfaces produced by chemical and topographic patterning. *Tissue Eng.* 2007, 13, 1879.
- [6]. Bettinger, C. J.; Langer, R.; Borenstein, J. T. Engineering substrate topography at the micro- and nanoscale to control cell. *Angew. Chem., Int. Ed. Engl.* 2009, 48, 5406.
- [7]. Martinez, E.; Engel, E.; Planell, J. A.; Samitier, J. Effects of artificial micro- and nanostructured surfaces on cell behaviour. *Ann. Anat.* 2009, 191, 126.
- [8]. Lord, M. S.; Foss, M.; Besenbacher, F. Influence of nanoscale surface topography on protein adsorption and cellular response. *Nano Today* 2010, 5, 66.
- [9]. Strobl, G. R. *The Physics of Polymers*, 2nd ed.; Springer-Verlag: Berlin, Germany, 1997; p 148.

- [10] .Keith, H. D. Banding in spherulites: Two recurring topics. *Polymer* 2001, 42, 9987.
- [11] .Lotz, B.; Cheng, S. Z. D. A critical assessment of unbalanced surface stresses as the mechanical origin of twisting and scrolling of polymer crystals. *Polymer* 2005, 46, 577.
- [12] .Cai, L.; Wang, S. *Polymer* 2010, 51, 164.

Chapter IV Melt Rheological Properties of Linear and Star-PCL Samples

4.1 Introduction

PCL is an FDA-approved biodegradable polymer with good biocompatibility. It can be degraded by hydrolysis of its ester linkages in physiological conditions and has received extensive attention such as being used as a temporary joint spacer and tissue-engineered skin [1,2].

Rheology behavior plays a very important role in polymer processing, operations and the viscoelasticity of polymer melts are mainly influenced by the molecular weight and distribution, temperature, and shear rate. Modeling the change in viscoelastic properties has great importance in predicting the flow behavior in different melt processing conditions. Therefore, it is necessary to have a better understanding on the detailed rheological properties of PCL [3].

Rheology is known as the study of deformation and flow of materials. Specifically flow is analyzed when forces act upon the material causing it to flow. Rheology and fluid mechanics are share similar concepts; however, rheology is concerned with all states of matter including solids, liquids, and gases whereas, fluid mechanics is only concerned with liquids. Also rheology studies focus on macroscopic properties but not molecular structure. Rheology is important to polymer analysis as it allows us to decipher viscoelastic properties of polymers which ultimately leads to mathematical modeling of polymers. Rheology is geared towards examining and studying “nonclassical” theories of viscosity, elasticity and non-Newtonian fluid mechanics. Rheology is effectively used to generate theories of which are not accurately described by classical mechanics. In order to study rheology, a rheometer is used as it effectively characterizes the flow of liquids, suspensions, and slurries with a response to applied external forces. There are several types of rheometers but, they can be classified into two categories: one being rotational/shear rheometers which are used to apply extensional stress and strain to materials and another one being extensional rheometers which are used to apply extensional stress and strain to materials.

Rheometers can also be used to determine pseudoplasticity where shear thickening and shear thinning occurs in these materials. It is known that polymers show a strong dependence of viscoelastic properties on temperature. Due to this, the elastic modulus is usually influenced by load time and response time. With these factors in mind, the time-temperature superposition is an important concept to consider as it implies that the response time function of elastic moduli at varied temperatures resembles the same shape of the same functions of adjacent temperatures.

The rheological properties of 4-arm and 6-arm PCL-OH with different molecular weights were determined by using the strain-controlled rheometer (RDS-w, Theometric Scientific). This work focused on understanding the zero shear viscosity dependence on temperature, molecular weight and shear rate. And the results were compared with linear ones.

4.2 Experiment

4.2.1 Material used in the experiment

Except for the four and six arm PCL-OH that were synthesized in the previous work, additional fifteen linear samples with Mw ranging from 1K to 773K were used in the experiment.

PCL144k (Mw = 144k g/mol), PCL69k, PCL24k, PCL5.2k, PCL3.3k and PCL1.2k were purchased from the Sigma-Aldrich. Other linear PCL samples were synthesized via the ring-opening polymerization in our lab previously.

4.2.2 Thermal characterization

Thermal properties of the linear PCL samples were determined by using DSC measurements on a Perkin Elmer Diamond differential scanning calorimeter in a nitrogen atmosphere. Samples were first heated from room temperature to 100°C and then cooled down to -90°C at a cooling rate of 5°C/min. After the pretreatment to get the same thermal history, a following heating run was performed from -90°C to 100°C at a heating rate of 10°C/min. DSC scans for the last cooling and

heating runs were recorded for analysis and the results were analyzed by the METTLER software in the instrument.

4.2.3 Rheological properties

The rheological properties of the samples were performed at 60, 80, 100, 120 and 140°C with a small strain (about 1%) with an 8 mm diameter parallel plate flow cell and a gap of about 0.5mm. While performing the experiment dynamic frequency sweep mode was used in order to measure the storage modulus (G') and the loss modulus (G'') and the zero shear viscosity was measured from the Newtonian region at low frequencies with the frequency range of 0.5-100rad/s.

4.3 Results and discussion

The DSC curves of linear PCL samples are shown in Figure 4-1. The molecular weight, PDI, and thermal properties of all the samples used in this experiment are summarized in Table 4-1.

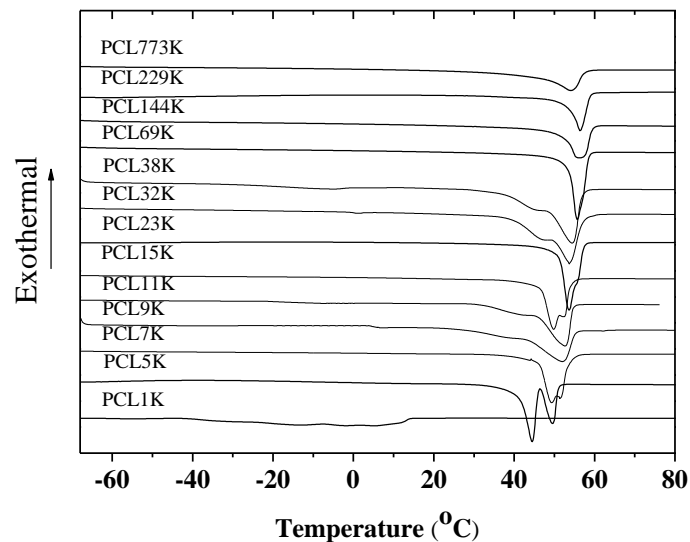


Figure 4-1 DSC curves of linear PCL samples with different molecular weights.

Linear PCL samples with weight-average molecular weights (M_w) varying from 1.2 to 774 kg/mol and the PDI of most PCL samples were between 1.1 and 1.5 except for the 2.1 of PCL774k sample. For the thermal properties shown in Table 4-1 and Figure 4-1, there were multiple melting peaks for PCL 5.2k, 3.3k, 1.2k and most 4,6arm samples because they were synthesized using a ring-opening polymerization while there was one melting temperature for other PCL samples, which was reported previously in our lab [3-6]. When the molecular weight increased, T_m for PCL increased up to 56.3°C for PCL229k. The crystallinity was calculated by the equation $crystallinity\% = \Delta H_m / (\phi_{PCL} \Delta H_m^c)$ Where $\Delta H_m^c = 135 J / g$ for PCL [2].

Table 4-1 Molecular characteristics and thermal properties of the linear, 4 and 6-arm PCL-OH

PCL-OH Polymer	M_n (g/mol)	M_w (g/mol)	PDI	Thermal properties				
				T_c (°C)	$T_{m,1}$ (°C)	$T_{m,2}$ (°C)	ΔH_m (J/g)	χ_c (%)
2-773K	365900	773900	2.1		54.1		46.6	34.5
2-229K	173800	229400	1.3		56.3		50.0	37.1
2-144K	97700	144200	1.5		56.0		55.5	41.1
2-135K	91700	135600	1.5		---		---	---
2-69K	46940	69130	1.5		55.4		67.2	49.8
2-42K	38280	42010	1.1		---		---	---
2-38K	35050	38140	1.1		54.1		69.0	51.1
2-32K	26550	32230	1.2		53.7		69.3	51.3
2-23K	17180	23980	1.4		53.4		72.2	53.5
2-15K	11050	15160	1.4		52.6		71.1	52.7
2-11K	10460	11850	1.1		52.5		70.8	52.4
2-9K	6570	9740	1.5		52.2		70.3	52.1
2-7K	5270	7120	1.4		51.4		70.0	51.9
2-5K	3470	5200	1.5		44.5	49.5	68.3	50.6
2-1K	1080	1180	1.1		5.5		25.3	18.7
4-8K	8450	9680	1.1	16.6	41.1	46.5	77.8	58.5
4-10K	9250	10300	1.1	21.0	45.8	49.4	76.6	57.5
4-14K	14200	15700	1.1	24.2	49.7	52.8	75.3	56.3
4-19K	19400	22900	1.1	25.0	51.6	54.3	80.5	60.0
4-25K	28100	36600	1.3	31.4	53.6	55.8	78.5	58.5
6-10K	9990	10900	1.1	15.1	39.8	44.8	76.2	57.9
6-13K	12800	14300	1.1	21.8	45.1	48.3	75.3	56.8
6-15K	14800	16800	1.1	21.5	42.9	48.8	78.7	58.3
6-20K	20600	25000	1.2	27.3	47.8	51.4	79.4	58.8
6-30K	30900	35600	1.2	31.6	49.2		73.7	54.6

The crystallinity first increased from 18.7% to 53.5% with increasing the weight-average molecular weight from 1.2 to 24 kg/mol and then decreased from 24 to 774 kg/mol because it was more difficult for PCL samples with sufficiently high molecular weights to reorganize into a more ordered structure. Compared with linear ones, the 4 and 6-arm samples had higher crystallinities, which were ranging from 54.6% to 60.0%

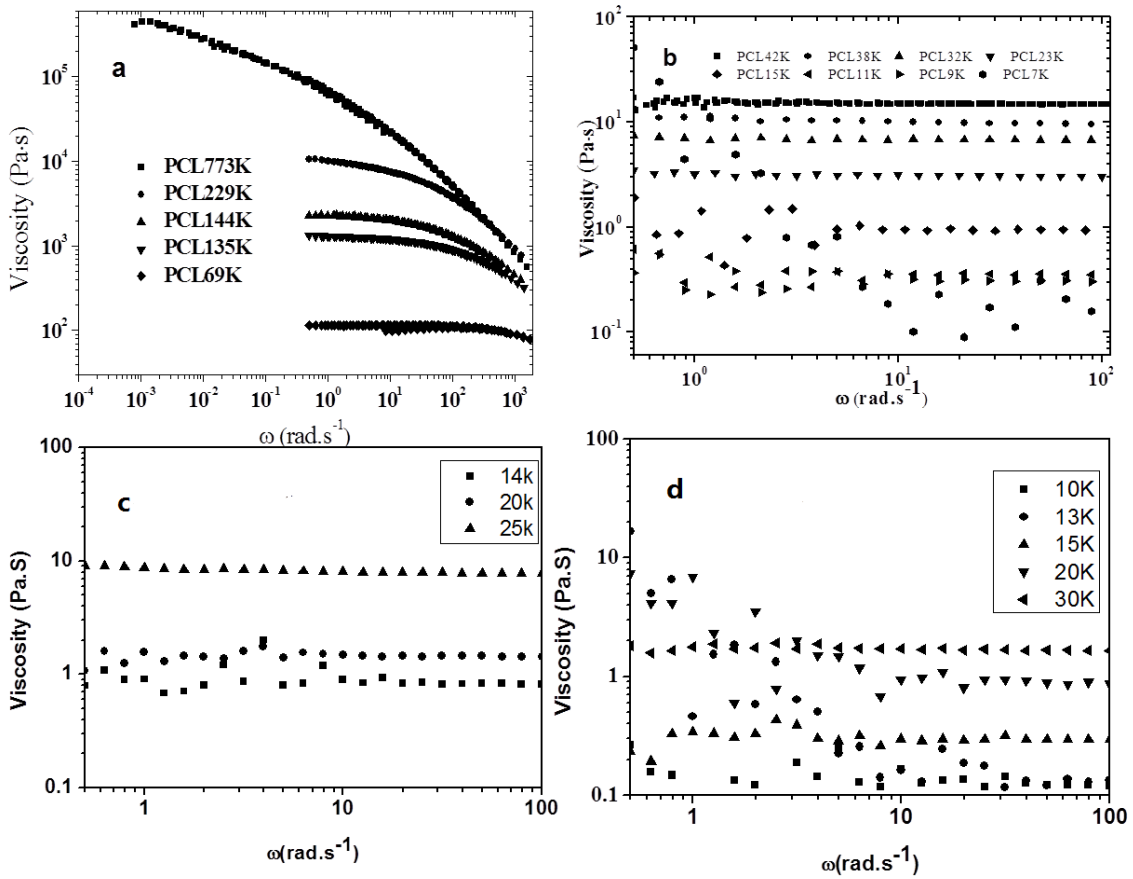


Figure 4-2 Strain rate dependence on the viscosity of (a) linear PCL samples with high molecular weight, (b) linear PCL samples with low molecular weight, (c) 4-arm PCL samples (d) 6-arm PCL samples, measured at 140°C.

Except for some samples with small molecular weights whose stable data could not be collected at 140°C, zero shear viscosity data of other samples were collected and plotted in Figure 4-2.

Shear thinning was observed in the linear samples when the molecular weight is over 69K, which means with the increase of shear rate, the decrease of zero viscosity were observed. Other sample behaved as a very good Newtonian Liquid. The zero-shear viscosity increases with the increase of Mw. The increased branches decrease the shear viscosity when the molecular weights are same. This is because each arm has fewer segments when the branch number is increased.

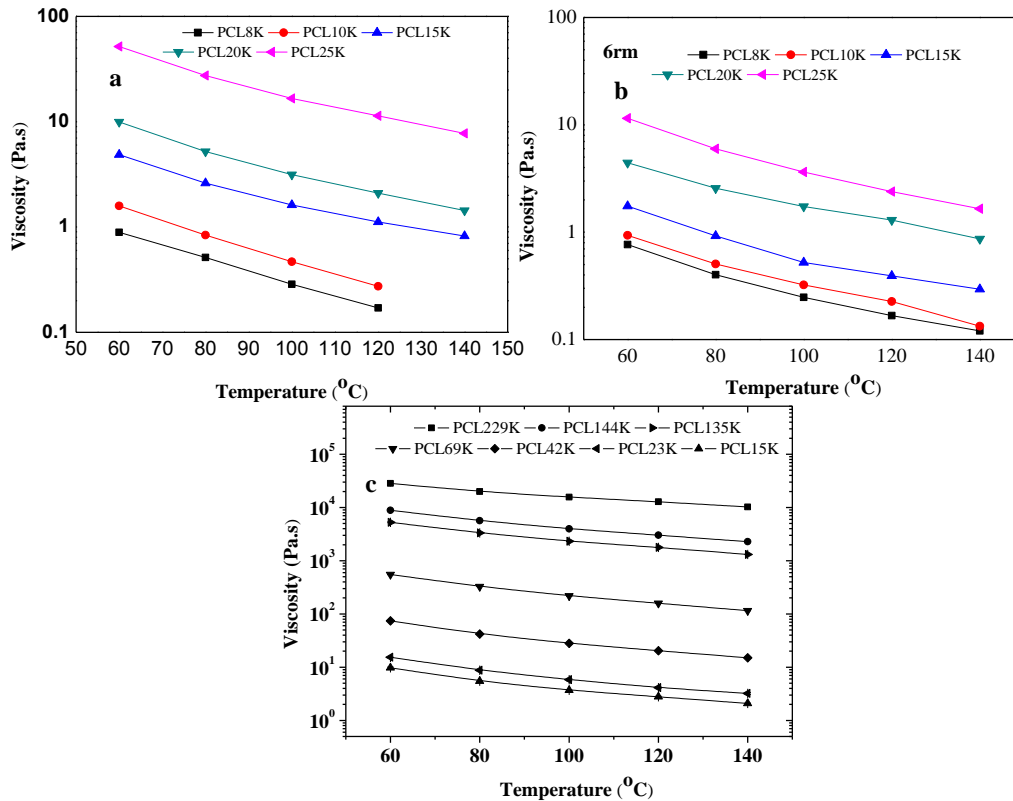


Figure 4-3 Temperature dependence on zero-shear viscosity of (a) 4-arm samples, (b) 6-arm samples and (c) linear samples measured at 140°C

The temperature dependence on zero-shear viscosity of the 4-arm, 6-arm and linear samples are shown in Figure 4-3. From the curves we could see that the curves with the viscosity are negatively correlated with the temperature, and at the same temperature, samples with higher molecular weight have higher viscosities.

The molecular weight dependence of zero-shear viscosity of 4arm and 6arm samples at different temperatures and the compared results with linear samples at 140°C are shown in Figure 4-4.

The slopes of the molecular weight dependence of viscosity are marked on the curves. As shown in the figure, for linear samples, there is a critical molecular weight 7K, after where the molecular weight dependence of shear viscosity behaved differently. This is because before the

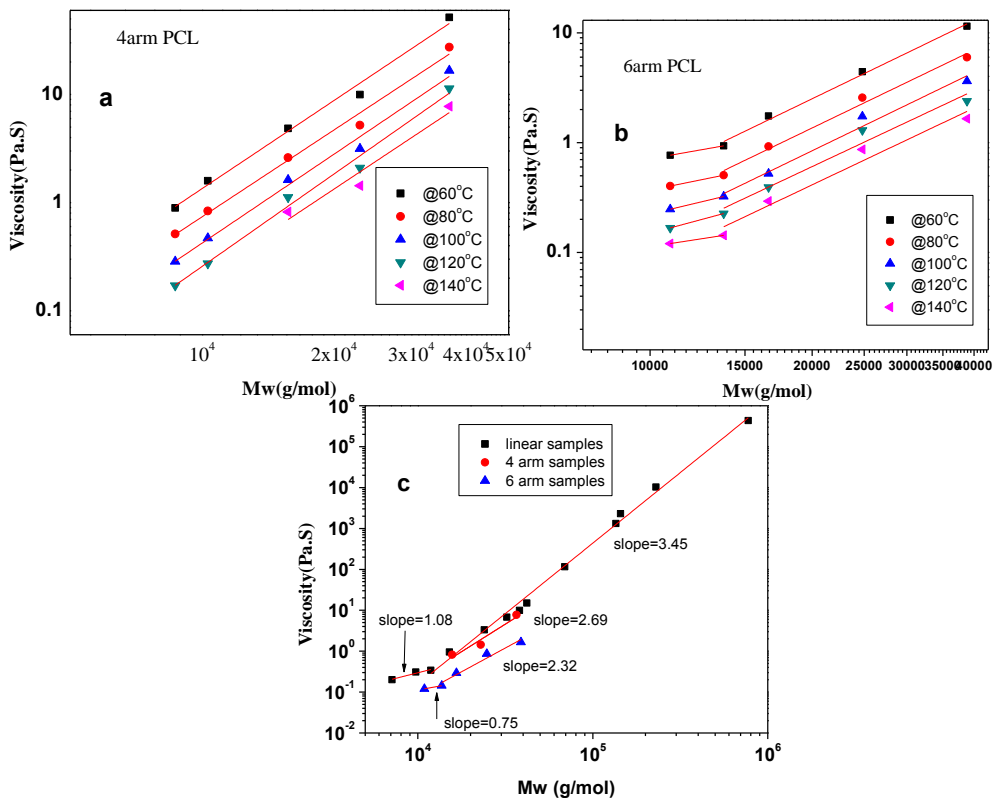


Figure 4-4 Molecular weight dependence on zero-shear viscosity of (a) 4 arm and (b) 6 arm samples at different temperatures and the compared results with (c) linear samples at 140°C

critical molecular weight, it is unentangled region and after this point, the polymer behaves as an entangled polymer.

The power law exponents of the unentangled and entangled regions were 1.0 and 3.5, consistent with the experimental findings of 1.08 and 3.45 for the linear polymers. The critical points were not observed in the 4 arm curves, more data points at lower molecular weight are needed to explore the power law. The critical points were observed at about 15K in the 6 arm curves, with a slope of about 1. In the entangled region, 4 arm and 6 arm samples obey a lower dependent factor because for star like polymers, the zero shear viscosity depended on the Molecular weight of each branch.

4.4 Conclusion

The linear samples obey the power law both on entangled and unentangled regions. More data points for 4 arm and 6 arm samples are needed to explore the molecular weight dependence in the unentangled region. The PCL-CH₃ and PCL-COOH samples were also used for the rheology tests to explore the functional group influence on polymer segments movements. No big differences were observed.

References

- [1]. Wang, S.; Lu, L.; Gruetzmacher, J. A.; Currier, B. L.; Yaszemski, M. J. *Macromolecules* 2005, 38, 7358.
- [2]. Wang, S.; Lu, L.; Gruetzmacher, J. A.; Currier, B. L.; Yaszemski, M. J. *Biomaterials* 2006, 27, 832.
- [3]. Gimenez, J.; Cassagnau, P.; Fulchiron, R.; Michel, A. *Macromol Chem Phys* 2000, 201, 479.
- [4]. O'Connell, C.; Sherlock, R.; Ball, M. D.; Aszalos-Kiss, B.; Prendergast, U.; Glynn, T. J. *Appl. Surf. Sci.* 2009, 255, 4405.
- [5]. Lampin, M.; Warocquier-Clerout, R.; Legris, C.; Degrange, M.; Sigot-Luizard, M. *F. J Biomed Mater Res.* 1997, 36, 99.
- [6] Harnett, E. M.; Alderman, J.; Wood, T. *Colloids and Surfaces B: Biointerfaces* 2007, 55, 90.

**Chapter V Cytotoxicity Test and in Vitro Cell Study of the Star-PCL
Samples Using Smooth Muscle Cells**

5.1 Introduction

After new polymers were synthesized, cytotoxicity evaluation should be taken in order to make sure the samples could be used for cell study. In this chapter, the cytotoxicity evaluation was performed by harvesting the SMCs. In vitro cell attachment and proliferation study were performed by harvesting SMCs on crystallized PCL with different functional groups.

5.2 Experiment

5.2.1 PCL sample preparation

All the 50 samples were used to perform the cytotoxicity tests. Before the tests, PCL samples were sterilized by immersing into 70% ethanol solution, and then dried in the vacuum dryer.

Only 4-25K and 6-30K PCL with different functional groups were used for in vitro cell attachment and proliferation study. The samples were crystallized at 37°C and sterilized by exposing under UV light for 12h.

5.2.2 Smooth Muscle Cells (SMCs)

Rat Smooth Muscle Cells isolated from adult rats aorta rats could be used for angiogenesis, atherosclerosis and cardiovascular research. The cell culture of SMCs were talked about in Charles' work [1]. SMCs were cultured in vitro by using culture medium consisting of Dulbecco's Modified Eagle Medium (DMEM), combined with 10% fetal bovine serum (FBS, Sera-Tech, Germany) and 1% penicillin/streptomycin (Gibco). Culture medium was placed into a polystyrene flask and SMCs were plated. Prior to seeding, the cell suspension was then incubated in a 5% CO₂, 95% relative humidity incubator at 37°C. Subcultures of SMCs were performed at approximately 80% confluency. Trypsin with a concentration of 0.025% was used to detach the cells from the bottom of the polystyrene flask.

5.2.3 Cytotoxicity tests

The procedures of the cytotoxicity tests were talked about in Lei's work [2]. Cytotoxicity evaluation was performed by harvesting SMCs in a 24-well plate at a density of about 15,000 cells/cm² in 1mL of primary medium. The suspension wells with a membrane were used to put PCL powders, as a result, only culture medium and possible toxic substance could go through the membrane. 0.1g sterilized sample was put into each well. The cells were kept in the incubator for 1, 2, and 4 days. Wells seeded with SMCs at the same density in the absence of complexes were used as positive controls and empty wells were used as negative controls. A colorimetric cell metabolic assay (Cell Titer 96 Aqueous One Solution, Promega, Madison, WI) based on the MTS tetrazolium compound was used to evaluate the number of viable cells, which could be correlated to the UV absorbance at 490 nm measured on a microplate reader (Spectra Max Plus 384, Molecular Devices, Sunnyvale, CA).

5.2.4 In vitro cell attachment and proliferation

SMCs were seeded on the polymer substrates at a density of 1.5×10^4 cells/cm². The negative control was the empty TCPS well and the positive control was TCPS seeded with cells. The seeded substrates were then incubated for 4 h to determine cell attachment and 1, 2, 4 days to determine proliferation. A microplate reader at 490 nm (Spectra Max Plus 384, Molecular Devices, Sunnyvale, CA) was used to determine the cell numbers obtained from the adsorption values of the MTS assay, (Cell Titer 96 Aqueous One Solution, Promega, Madison, WI) and a standard curve constructed from known cell numbers. Culture medium was removed from the wells containing SMC seeded substrates and the polymer substrates were washed twice with PBS after the cells were cultured in a 5% CO₂ and 95% relative humidity atmosphere at 37 °C for 4 h, 1, 2 and 4 days.

For fluorescent imaging, the attached cells were fixed in 4% paraformaldehyde (PFA) solution for 10 min. After fixation, the PFA was removed and PBS was used to wash the cells twice. Cells were permeabilised with 0.1% Triton X-100 for 10-20 min. The cytoplasm filaments were stained with rhodamine-phalloidin (RP) and incubated for 1 h at 37 °C. After incubating, 4',6-diamidino-2-phenylindole (DAPI) was used to stain the cell nuclei. SMC images were acquired with an Axiovert 25 light microscope (Carl Zeiss, Germany). Proliferation index (PI) was quantified by dividing the cell number at day 4 by the cell number at day 1.

5.3 Results and discussion

The normalized cell numbers in the tested wells compared with those in the positive control wells after 1, 2 and 4 day are shown in Figure 5-1. From the figure we could see that there was no big difference on cell numbers between tested wells and positive control wells. That's to say, all the polymers are not harmful for the SMCs and can be used in cell studies.

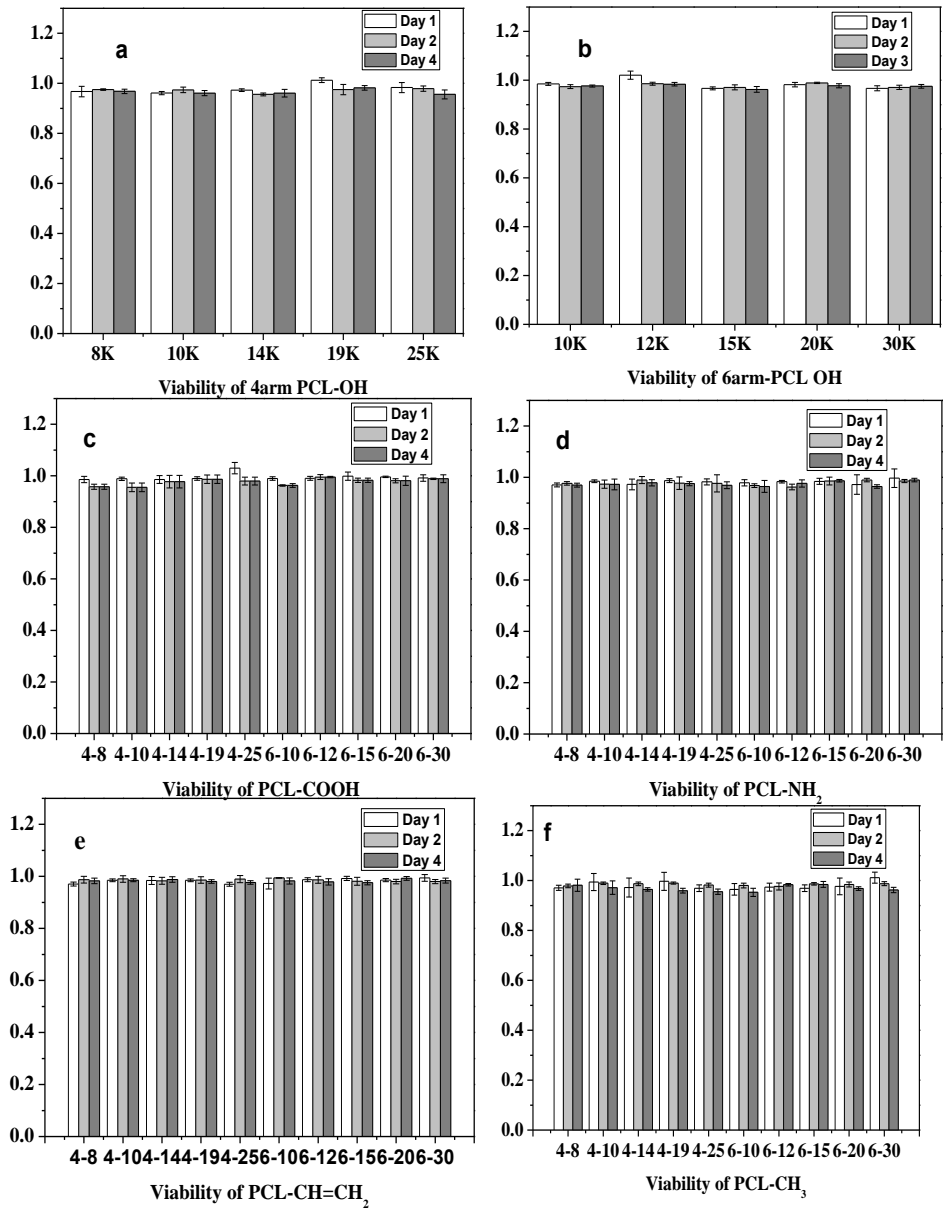


Figure 5-1 Normalized cell numbers after 1, 2 and 4 days for (a) 4-arm PCL-OH (b) 6-arm PCL-OH (c) PCL-COOH (d) PCL-NH₂ (e) PCL-acrylate (f) PCL-CH₃ samples.

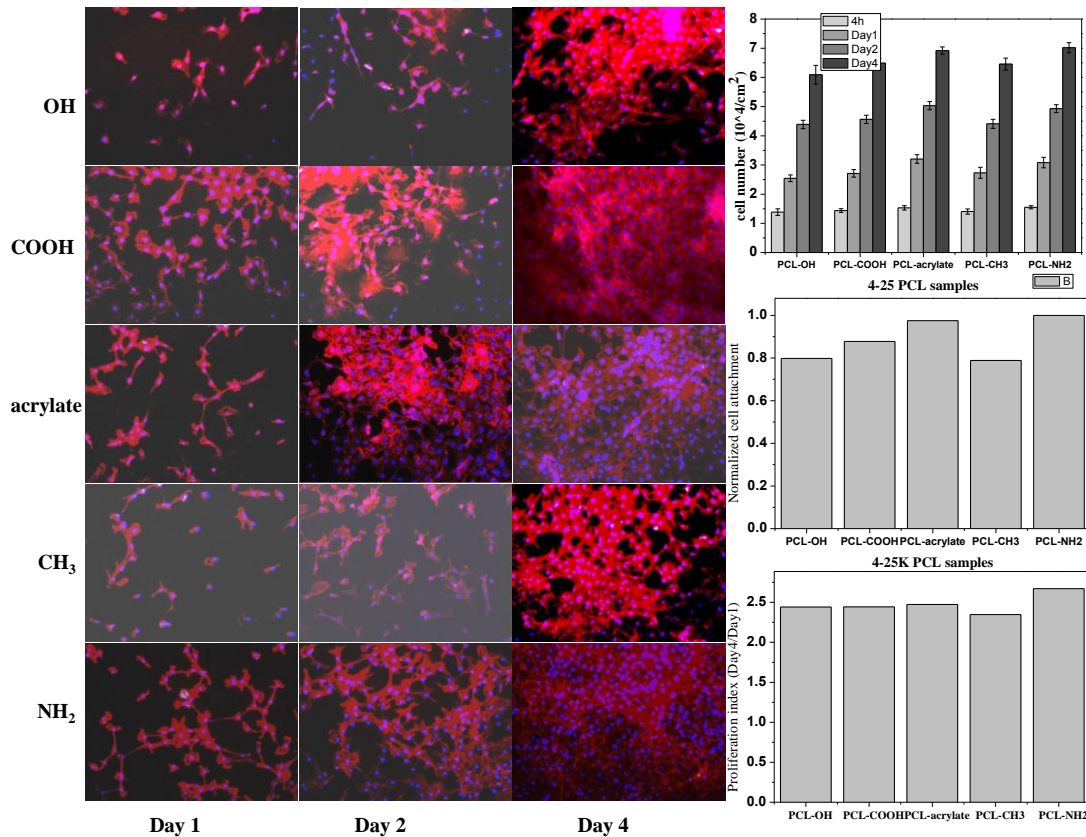


Figure 5-2 SMCs cell attachment and proliferation on crystallized 4arm-25K PCL films.

The cell numbers and the fluorescent images stained with rhodamine-phalloidin (red) and DAPI (blue) on functional group end-capping PCL film at days 1, 2, and 4 post-seeding are shown in Figure 5-2. Normalized cell attachment at 4h and proliferation index (Day 4 cell number/Day 1 cell number) are calculated and the results are also shown in Figure 5-2. As the results showed, the amino group PCL enhanced both on SMCs attachment and proliferation. The carboxyl and acrylate group PCL increased the cell attachment a little bit. The methyl groups did not change the polymer interaction with cells.

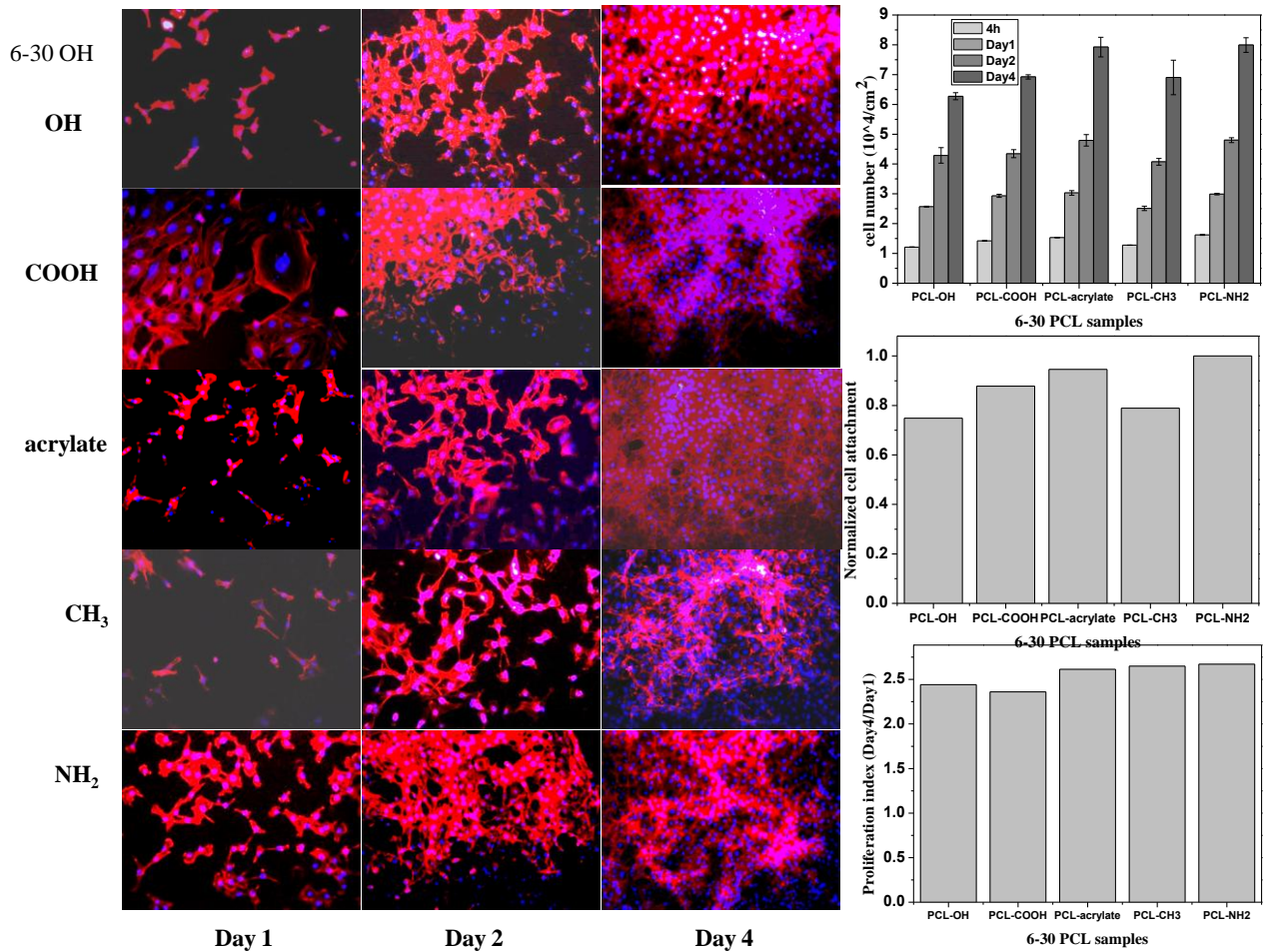


Figure 5-3 SMCs cell attachment and proliferation on crystallized 6arm-30K PCL films.

Same trend were observed when 6arm-30K crystallized samples were used as the cell growing substrate, cell images, cell numbers, normalized attachment and Proliferation index are shown in Figure 5-3. Compared with the results of 4arm-25K, samples, the attachment enhancement is more significant.

5.4 Conclusion

According to the cytotoxicity test results, all the studied samples were not toxic and can be used in cell study.

The in vitro cell study showed that the PCL-NH₂ samples enhanced both on SMCs attachment and proliferation. The PCL-COOH and PCL-acrylate samples increased the cell attachment a little bit. The PCL-CH₃ did not change the polymer interaction with cells a lot.

The enhancement of attachment and cell numbers for 6-arm samples are more significant than that of 4-arm samples.

More cell studies could be applied to find out how different molecular weights, differern surface morphologies could influence cell behavior and further studies on SMC functions such as focal adhesions, integrin/gene/protein expression, and filament could be applied.

References

- [1] Sprague, Charles Henley, "Biodegradable Nano-Hybrid Polymer Composite Networks for Regulating Cellular Behavior." Master's Thesis, University of Tennessee, 2015.
- [2] Cai, Lei, "Modulation of Bone and Nerve Cell Behavior Using Biodegradable Polymer Networks. " PhD diss., University of Tennessee, 2012.

Chapter VI Conclusion and Further Work

In chapter II, 4-arm and 6-arm star-like PCL with different molecular weight and functional groups were synthesized with structure confirmed by GPC, ATR and NMR. Based on the NMR spectra, the conversion percentage of the functional groups could be calculated. The thermal properties of the samples were determined by using DSC.

After the structure were determined, flat samples were prepared by the hot press and the contact angle tests of three fluids were performed. Based on the contact angles, surface energies could be calculated.

For further work of this chapter, X-ray photoelectron spectroscopy (XPS) could be used to further determine the density of functional groups on the PCL surfaces.

In chapter III, different functional group end-capping PCL samples were used to study the influence of functional groups and different crystalline temperature on crystalline morphologies. The crystalline morphologies were observed under POM and banded structure were observed when the PCL-CH₃ and PCL-acrylate samples were crystallized at 50°C.

Formation of banded spherulites can be attributed to polymer lamellar twisting in crystal growth induced by the strong surface stress of the lamellae and impeded crystal growth rate. The substrate could influence the crystalline morphologies by changing the crystal growth rate. Even though no banded structure were observed in my work, this part worth further study to find out how could the substrate influence the crystallization.

In my work, POM images were taken only when the spherulites stopped growing, crystallization kinetics could be studied by taking the images every specific time for further understanding the crystalline procedure. Atomic force microscope (AFM) could also be used to further study the roughness of the crystallized surface.

In chapter IV, the molecular weight and temperature dependence on zero-shear viscosity of 4 and 6-arm PCL were studied and compared with the linear samples. Most of my 4-arm and 6-arm samples are in the entangled region, for further study, more star-like polymers with lower molecular weights are needed to explore the molecular weight dependence for branched polymer in the unentangled region.

In chapter V, in vitro cell studies were performed by using SMCs cultured on the crystallized PCL films. The amino groups enhanced both on SMCs attachment and proliferation. The carboxyl and acrylate groups increased the cell attachment a little bit. The methyl groups did not change the polymer interaction with cells very much.

It was talked about that cell behaviors could be influence by surface mechanics, surface morphological and chemical features. In chapter V, only PCL samples with different functional groups were used to study the chemical influence. The stiffness of the samples depends on the molecular weight. Flat samples with different molecular weight could be prepared to study the surface mechanic influence. Samples with different surface morphologies could be prepared by changing the crystalline temperature to further study the morphology influence.

Except for the cell attachment and proliferation, further studies on SMC functions such as focal adhesions, integrin/gene/protein expression, and filament could be also applied.

Vita

Qingya Zeng was born in Zaozhuang, Shandong, P.R.China in 1990. He attended Shandong University from 2008 to 2012, where he received a B.S degree from the College of Material Science and Engineering with a major in Polymer Material Science and Engineering. In the fall of 2013, he enrolled at the University of Tennessee, in the Department of Materials Science and Engineering (MSE) and focused on polymer. He received a Master of Science Degree in Materials Science and Engineering from the University of Tennessee in May 2017.